

# Assessment of the Electronic Factors Determining the Thermodynamics of “Oxidative Addition” of C–H and N–H Bonds to Ir(I) Complexes

David Y. Wang,<sup>†</sup> Yuriy Choliy,<sup>†</sup> Michael C. Haibach,<sup>†</sup> John F. Hartwig,<sup>‡</sup> Karsten Krogh-Jespersen,<sup>\*,†</sup> and Alan S. Goldman<sup>\*,†</sup>

<sup>†</sup>Department of Chemistry and Chemical Biology, Rutgers, The State University of New Jersey, New Brunswick, New Jersey 08903, United States

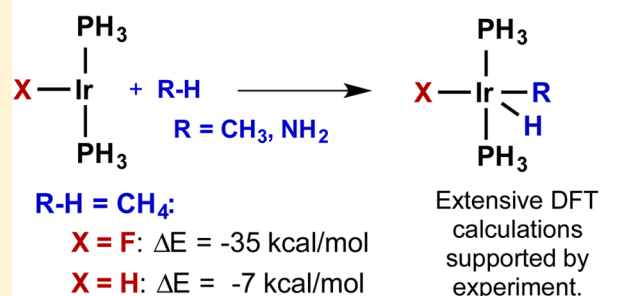
<sup>‡</sup>Department of Chemistry, University of California, Berkeley, Berkeley, California 94720-1460, United States

## Supporting Information

**ABSTRACT:** A study of electronic factors governing the thermodynamics of C–H and N–H bond addition to Ir(I) complexes was conducted. DFT calculations were performed on an extensive series of *trans*-(PH<sub>3</sub>)<sub>2</sub>IrXL complexes (L = NH<sub>3</sub> and CO; X = various monodentate ligands) to parametrize the relative  $\sigma$ - and  $\pi$ -donating/withdrawing properties of the various ligands, X. Computed energies of oxidative addition of methane to a series of three- and four-coordinate Ir(I) complexes bearing an ancillary ligand, X, were correlated with the resulting ( $\sigma_X$ ,  $\pi_X$ ) parameter set. Regression analysis indicates that the thermodynamics of addition of methane to *trans*-(PH<sub>3</sub>)<sub>2</sub>IrX are generally strongly *disfavored* by increased  $\sigma$ -donation from the ligand X, in contradiction to widely held views on oxidative addition. The trend for oxidative addition of methane to four-coordinate Ir(I)

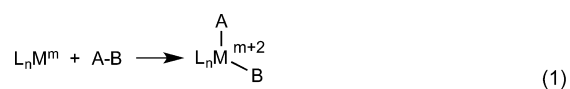
was closely related to that observed for the three-coordinate complexes, albeit slightly more complicated. The computational analysis was found to be consistent with the rates of reductive elimination of benzene from a series of isoelectronic Ir(III) phenyl hydride complexes, measured experimentally in this work and previously reported. Extending the analysis of ancillary ligand energetic effects to the oxidative addition of ammonia to three-coordinate Ir(I) complexes leads to the conclusion that increasing  $\sigma$ -donation by X also *disfavors* oxidative addition of N–H bonds to *trans*-(PH<sub>3</sub>)<sub>2</sub>IrX. However, coordination of NH<sub>3</sub> to the Ir(I) center is disfavored even more strongly by increasing  $\sigma$ -donation by X, which explains why the few documented examples of H–NH<sub>2</sub> oxidative addition to transition metals involve complexes with strongly  $\sigma$ -donating ligands situated *trans* to the site of addition. An orbital-based rationale for the observed results is presented.

**“Oxidative” addition to Ir(I) strongly disfavored by more electron-donating ancillary ligand X**



## INTRODUCTION

Oxidative addition (OA) is perhaps the most characteristic reaction of transition metal complexes.<sup>1,2</sup> It is a key step in the majority of transition-metal-catalyzed reactions including hydrogenations,<sup>3,4</sup> carbonylations,<sup>5,6</sup> and cross-couplings.<sup>7–9</sup> The reaction typically comprises cleavage of a covalent A–B bond with concomitant formation of metal–A and metal–B bonds and is thus commonly viewed as a formal two-electron oxidation of a metal center (eq 1).



The metal–ligand bonds formed can have significant covalent character, however, and thus caution has been urged in adopting a literal interpretation of the oxidative addition formalism. Among the most notable examples of such

admonitions, Saillard and Hoffman,<sup>10</sup> Low and Goddard,<sup>11</sup> and Koga and Morokuma<sup>12</sup> have all emphasized that oxidative addition involves the movement of electron density both from the ligand to the metal and from the metal to the ligand. Crabtree has proposed that, in some systems, reactions of the type illustrated by eq 1 are even best viewed as reductive additions.<sup>13</sup> Nevertheless, the assumption that oxidative addition is favored by metal centers that are more electron-rich, and thus by ligands that are more strongly electron-donating, remains deeply ingrained in the conventional understanding and practice of organometallic chemistry.<sup>14–17</sup> Accordingly, it is common to use ligands with increased electron-donating ability to promote the kinetics and thermodynamics of oxidative addition<sup>18–20</sup> and, conversely, to use those with increased electron-withdrawing properties to

Received: September 9, 2015

Published: December 10, 2015

promote the kinetics and thermodynamics of the microscopic reverse reaction, reductive elimination (RE).<sup>21–23</sup>

Oxidative addition of C–H bonds to metal centers has attracted particularly intense interest since the discovery of this reaction with alkanes.<sup>24</sup> Given the ubiquity of the C–H bond and its status as a prototypical covalent bond, it has become an archetypal substrate for the oxidative addition of covalent bonds. In at least one respect, the C–H bond is more representative and better suited for this role than the simplest covalent bond, that of dihydrogen, because the addition of dihydrogen often results in products with at least partial character of a  $\sigma$ -dihydrogen complex rather than a true product of OA.<sup>25–33</sup>

Although N–H bonds are generally considered much more reactive than C–H bonds, few examples of simple OA of amines to metal centers have been reported. Examples involving addition of the simplest such addendum, ammonia, are particularly limited.<sup>34–42</sup> We reported that the aryl-pincer ligated fragment (PCP)Ir (PCP =  $\kappa^3$ -C<sub>6</sub>H<sub>3</sub>-2,6-[CH<sub>2</sub>P(*t*-Bu)<sub>2</sub>]<sub>2</sub>) underwent oxidative addition of the N–H bond of aniline, but not ammonia; however, the complex of a more electron-donating aliphatic-PCP ligand, ( $\kappa^3$ -CH[C<sub>2</sub>H<sub>4</sub>P(*t*-Bu)<sub>2</sub>]<sub>2</sub>), underwent the oxidative addition of ammonia.<sup>36</sup> This observation appeared to be consistent with the generally accepted view regarding the favorable effect of increased ligand electron-donating ability on oxidative addition.

Oxidative additions to four-coordinate complexes with a d<sup>8</sup> electron configuration, including those of Rh(I) and Pt(II), are particularly common, and addition to square planar Ir(I) is generally considered the classic example of this reaction.<sup>14–17</sup> Indeed, the designation of addition of substrates not normally considered to be oxidants (e.g., addition of H<sub>2</sub>) as being “oxidative” originated in the context of addition to square planar Ir(I); this perspective directly led to the tenet that such additions are favored by electron-donating ligands.<sup>43,44</sup>

Compared with the addition of H<sub>2</sub>, the addition of C–H bonds to four-coordinate d<sup>8</sup> complexes is more limited.<sup>45–48</sup> Three-coordinate Ir(I), as well as Rh(I) and Pt(II), however, play a central role in C–H addition chemistry.<sup>49</sup> Several theoretical studies of oxidative addition to three-coordinate Ir(I) and Rh(I) complexes have indicated that electron-donating ligands do not necessarily favor addition. Cundari calculated that the enthalpy of the oxidative addition of methane to *trans*-(PH<sub>3</sub>)<sub>2</sub>IrX (X = H, Cl) was significantly more favorable for (PH<sub>3</sub>)<sub>2</sub>IrCl ( $\Delta H = -41.6$  kcal/mol) than for (PH<sub>3</sub>)<sub>2</sub>IrH ( $\Delta H = -12.8$  kcal/mol).<sup>50</sup> Similarly, we reported that oxidative addition of H<sub>2</sub> to *trans*-(PH<sub>3</sub>)<sub>2</sub>MX complexes (X = Cl, Ph; M = Rh, Ir) was significantly more favorable for X = Cl than X = Ph ( $\Delta\Delta E = 24.3$  and 31.1 kcal/mol for M = Rh and Ir, respectively).<sup>51</sup> In both cases, oxidative addition to the complex with the more strongly electron-donating ligands (i.e., H<sup>−</sup> and Ph<sup>−</sup>) was less favorable than oxidative addition to the complex with the weakly donating chloride ligand. In contrast, we reported that, for a series of Y–PCP pincer complexes, in which Y is a *para*-substituent on the aryl backbone, increased electron donation from Y favored H<sub>2</sub> or C–H oxidative addition to three-coordinate (Y–PCP)Ir, although it disfavored addition to square planar (Y–PCP)Ir(CO). Because the effect of Y was transmitted from the *para*-position of the pincer aryl group, this electronic effect was recognized to be largely attributable to  $\pi$ -symmetry interactions.<sup>52</sup>

In several other studies, oxidative addition has been calculated to be more favorable for complexes bearing less

electron-donating ancillary ligands than for those bearing more electron-donating ancillary ligands; examples include systems based on three-coordinate Ir(I) and Rh(I)<sup>53–55</sup> and Ru(0).<sup>56</sup> To our knowledge, however, a comprehensive examination of the electronic effects of ancillary ligands on the thermodynamics of oxidative addition has not been conducted. Herein, we report a systematic approach, based on DFT calculations, to elucidate the electronic factors that influence the thermodynamics of the oxidative addition of C–H (methane) and N–H (ammonia) bonds to both three- and four-coordinate Ir(I) complexes. The rates of reductive elimination from a series of isoelectronic Ir(III) phenyl hydride complexes have been experimentally determined and found to be consistent with the computational analysis.

## ■ COMPUTATIONAL METHODS

All calculations used DFT methodology<sup>57</sup> as implemented in the Gaussian 03 and Gaussian 09 series of computer programs.<sup>58</sup> We employed the Perdew–Burke–Ernzerhof exchange–correlation functional (PBE) in all calculations.<sup>59</sup> For the model complexes 1–3, we applied the SDD relativistic, small-core effective potential and corresponding basis set to the Ir atom<sup>60</sup> and all-electron, valence triple- $\zeta$  plus polarization and diffuse function 6–311+G(d,p) basis sets to all nonmetal atoms.<sup>61–64</sup> For the calculations on experimental complexes 4–7 and related species, we used the LANL2DZ relativistic, small-core effective potential and the LANL2TZ basis set augmented by a diffuse d-type function (exponent = 0.07645) for Ir;<sup>65,66</sup> 6–311+G(d,p) basis sets for atoms bonded to Ir or contained in substrate molecules (e.g., CH<sub>4</sub>, NH<sub>3</sub>, or benzene); and valence double- $\zeta$  plus diffuse function 6–31+G basis sets for all other atoms. Complex geometries were optimized, often subject to imposed structural constraints. Stationary points on the potential energy surfaces were identified and characterized by normal-mode analysis. Electronic population indices were derived from the Natural Bond Orbital (NBO) analysis scheme developed by Weinhold et al.<sup>67,68</sup> and calculated using the software package NBO 5.G interfaced with Gaussian 03.<sup>69</sup>

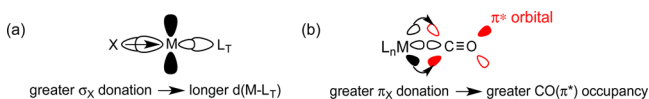
## ■ RESULTS AND DISCUSSION

**Parameterization of Ancillary Ligand Electronic Properties.** The effects of varying the nature of the ancillary ligands on the oxidative addition of C–H/N–H bonds to Ir(I) complexes were determined from a series of comparative calculations on small model complexes. To isolate solely the electronic effects, we chose to minimize steric contributions and focused on complexes with a (PH<sub>3</sub>)<sub>2</sub>IrX substructure (X = various monodentate ligands) in which the PH<sub>3</sub> groups were held mutually *trans*. Provided that ligand X is not unusually large, we can assume that steric interactions with the phosphines are negligible and, consequently, that the effects of varying X on the calculated reaction energies will be strictly attributable to electronic effects. The set of X ligands investigated features a wide range of  $\sigma$ - and  $\pi$ -type electronic properties and includes strongly  $\sigma$ -donating ligands (H<sup>−</sup>, Li<sup>−</sup>, Ph<sup>−</sup>, Me<sup>−</sup>); a weakly  $\sigma$ -donating ligand (pyrrolide); a strongly  $\sigma$ - and  $\pi$ -donating ligand (O<sup>2−</sup>); a strongly  $\sigma$ -donating and  $\pi$ -accepting ligand (BH<sub>2</sub><sup>−</sup>); ligands that are  $\pi$ -donating and weakly  $\sigma$ -donating (NH<sub>2</sub><sup>−</sup>, F<sup>−</sup>, OH<sup>−</sup>, OMe<sup>−</sup>); and a ligand that is weakly  $\sigma$ -donating and  $\pi$ -accepting (NO<sub>2</sub><sup>−</sup>). As described below, the computed electronic effects were separated into  $\sigma$  and  $\pi$  components and separately parametrized to yield substituent parameters designated  $\sigma_X$  and  $\pi_X$ , respectively.

The  $\sigma$ -donating ability of each substituent X was determined on the basis of its *trans*-influence. *Trans*-influence is a ground state effect in which the nature of a given ligand affects the

strength, and hence the length, of the bond between the metal and the ligand ( $L_T$ ) coordinated trans to that ligand.<sup>14,70</sup> If  $L_T$  binds solely to the metal center through  $\sigma$ -type interactions, then the length of the  $M-L_T$  bond presumably reflects the effective  $\sigma$ -donating ability of X (Scheme 1a).

**Scheme 1. (a) Trans-Influence of Ligand X on the  $M-L_T$  Distance; (b)  $\pi$ -Backbonding of Electron Density from a Metal to Formally Vacant, Antibonding  $\pi^*$  Orbitals of CO**



$NH_3$  was chosen as our prototypical trans ligand,  $L_T$ . The geometries of a series of *trans*-( $PH_3$ )<sub>2</sub>IrX( $NH_3$ ) complexes (**1-X**, Figure 1) were optimized to determine equilibrium Ir–N

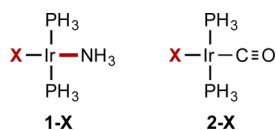


**Figure 1.** Model complexes used to determine electronic substituent effect parameters  $\sigma_X$  (**1-X**) and  $\pi_X$  (**2-X**).

bond distances. The model complexes were then constrained to rigorously maintain square planar geometries (angles between ligands were fixed at  $90^\circ$ ) to eliminate unusual perturbations to the geometry about the metal center. In addition, the orientation of some ligands ( $BH_2^-$ ,  $NH_2^-$ ,  $NO_2^-$ ,  $OH^-$ ,  $OMe^-$ ,  $Ph^-$ , and pyrrolide) were constrained to be coplanar with, or orthogonal to, the molecular plane of the complex (the plane defined by Ir and the central atoms of X and  $PH_3$  groups);<sup>71</sup> all remaining geometrical variables were allowed to freely optimize. Differences in the Ir–N bond distances between constrained and corresponding unconstrained complexes were typically quite small.<sup>72</sup> Optimized structural data for fully unconstrained complexes are available in the [Supporting Information](#).

The  $\sigma_X$  parameter was referenced relative to the Ir–N bond distance for **1-H**, as shown in eq 2. Ligands that cause the Ir–N bonds to be longer than the Ir–N bond of **1-H** are considered to be stronger  $\sigma$  donors than hydride and have positive  $\sigma_X$  parameter values, while ligands that cause the Ir–N bonds to be shorter have negative values of  $\sigma_X$ . The series of  $\sigma_X$  parameter values thus obtained is shown in Table 1. The rank order conforms well with conventional expectations. The  $\sigma_X$  values of methyl and phenyl, which are generally regarded as strong trans-influence ligands (comparable to hydride), are near zero ( $-0.015$  and  $-0.012$ , respectively), while the  $\sigma_X$  values of weakly  $\sigma$ -donating substituents such as fluoride and hydroxide are significantly negative ( $-0.146$  and  $-0.110$ , respectively). The  $\sigma_X$  values of only  $Li^-$ ,  $BH_2^-$ , and the dianionic ligands  $BH_3^{2-}$  (the isoelectronic analogue of  $CH_3^-$ ) and  $O^{2-}$  are calculated to be positive, indicating  $\sigma$ -donating abilities greater than that of  $H^-$ . The orientation of unsymmetrical ligands, e.g.  $BH_2^-$ ,  $NH_2^-$ , and  $OH^-$ , has only a very small effect on their  $\sigma_X$  values, but does have a large effect on their  $\pi$ -donating ability (see below); this difference is consistent with the respective symmetry of  $\sigma$ - and  $\pi$ -interactions, thus validating our method for the dissection of these effects.

**Table 1.** Calculated Electronic Substituent Parameters ( $\sigma_X$ ,  $\pi_X$ ); Ligands Rank Ordered by Values of  $\sigma_X$  (left) and  $\pi_X$  (right)<sup>a</sup>

X ligand	$\sigma_X$	$\pi_X$	X ligand	$\pi_X$	$\sigma_X$
$BH_3^{2-}$	0.235	0.072	$O^{2-}$	0.198	0.023
$BH_2^-, \parallel$	0.139	-0.061	$OMe^-, \parallel$	0.074	-0.113
$Li^-$	0.128	0.003	$OH^-, \parallel$	0.073	-0.113
$BH_2^-, \perp$	0.115	-0.013	$BH_3^{2-}$	0.072	0.235
$O^{2-}$	0.023	0.198	$NH_2^-, \parallel^b$	0.071	-0.072
$H^-$	0.000	0.000	$F^-$	0.046	-0.146
$Ph^-, \perp$	-0.012	-0.003	$OH^-, \perp$	0.019	-0.110
$CH_3^-$	-0.015	0.013	$OMe^-, \perp$	0.013	-0.106
$CF_3^-$	-0.033	-0.025	$CH_3^-$	0.013	-0.015
$NO_2^-, \parallel$	-0.071	-0.029	$NO_2^-, \perp$	0.005	-0.081
$NH_2^-, \parallel^b$	-0.072	0.071	$Li^-$	0.003	0.128
$NH_2^-, \perp^c$	-0.072	-0.001	$H^-$	0.000	0.000
$NO_2^-, \perp$	-0.081	0.005	$NH_2^-, \perp^c$	-0.001	-0.072
$OMe^-, \perp$	-0.106	0.013	$Ph^-, \perp$	-0.003	-0.012
pyrrolide, $\perp$	-0.108	-0.013	$BH_2^-, \perp$	-0.013	0.115
$OH^-, \perp$	-0.110	0.019	pyrrolide, $\parallel$	-0.013	-0.108
$OH^-, \parallel$	-0.113	0.073	$CF_3^-$	-0.025	-0.033
$OMe^-, \parallel$	-0.113	0.074	$NO_2^-, \parallel$	-0.029	-0.071
$F^-$	-0.146	0.046	$NH_3$	-0.054	-0.153
$NH_3$	-0.153	-0.054	$BH_2^-, \parallel$	-0.061	0.139

<sup>a</sup> $\parallel$  = coplanar with P–Ir–P axis.  $\perp$  = orthogonal to P–Ir–P axis. <sup>b</sup>H–N–Ir–P dihedral angles set to  $31.5^\circ$ . <sup>c</sup>H–N–Ir–P dihedral angles set to  $58.5^\circ$ .

$$\sigma_X = [(\text{computed Ir–N bond distance})_{1-X} - (\text{computed Ir–N bond distance})_{1-H}] / \text{\AA} \quad (2)$$

The  $\pi$ -donating or  $\pi$ -withdrawing ability of ligand X was determined from considerations of metal( $d_\pi$ )–ligand( $p_\pi$ ) backbonding.<sup>73</sup> The extent to which electron density is transferred from doubly occupied Ir  $d_\pi$ -orbitals into formally vacant CO( $\pi^*$ ) orbitals (Scheme 1b) in a series of four-coordinate *trans*-( $PH_3$ )<sub>2</sub>IrX(CO) complexes **2-X** (Figure 1) was quantified. To do so, we computed the electron occupancies (NBO population analysis) in the Lewis-type antibonding CO( $\pi^*_{pz-pz}$ ) orbital (the CO( $\pi^*$ ) orbital that is oriented parallel to the z axis, i.e., perpendicular to the X–P–Ir–P molecular plane).<sup>67,68</sup> At first, the geometries of **2-X** (X ligand set shown in Table 1) were fully optimized with no symmetry constraints imposed; the average Ir–CO bond distance from these calculations was found to be 1.868 Å. Geometries of carbonyl complexes **2-X** were then constrained to be rigorously square planar in the same manner as described above for ammine complexes **1-X**, and additionally, the Ir–CO bond distance was constrained to the length 1.868 Å. This latter constraint was imposed to address the concern that the trans-influence exerted by ligand X could affect the Ir–CO bond distance; any such effect on the bond distance would influence Ir( $d_\pi$ )–CO( $\pi^*$ ) orbital overlap, and hence it would influence electron occupancies of the CO( $\pi^*$ ) orbitals through a mechanism that is independent of the inherent  $\pi$ -donating or  $\pi$ -accepting characteristics of ligand X. The effect of varying the Ir–CO distance on the CO( $\pi^*_{pz-pz}$ ) orbital occupancies is illustrated in Table S-1 (Supporting Information) for complex **2-F** and is found to be small. Constraining the Ir–CO bond distance to the common value of 1.868 Å for all complexes eliminated this admittedly small but extraneous effect; computed differences in orbital occupancies can thus be safely



assumed to predominantly reflect differences in the degree to which X favors or disfavors  $\pi$ -donation from the iridium center.

The  $\pi_X$  substituent parameter is defined as shown in eq 3 and referenced to the CO( $\pi^*_{pz-pz}$ ) occupancy for 2-H. Ligands with positive values of  $\pi_X$  are considered to be  $\pi$ -donors, whereas ligands having a negative  $\pi_X$  value are considered to be  $\pi$ -acceptors. The trend in the  $\pi_X$  values (Table 1) is as expected. The dianionic  $\pi$ -donor  $O^{2-}$  has by far the largest  $\pi_X$  value.  $BH_2^-$  has the most negative value, but only when oriented in the plane of the Ir and other coordinating atoms; when oriented perpendicular to that plane the  $\pi_X$  value is close to zero.  $\pi$ -Donating ligands such as amido and methoxide have large, positive  $\pi_X$  values (0.071 and 0.074, respectively) when oriented in or nearly in the coordination plane, but have much smaller  $\pi_X$  values when rotated by  $90^\circ$ .

$$\pi_X = (\text{computed CO}(\pi^*_{pz-pz}) \text{ occupancy})_{2-X} - (\text{computed CO}(\pi^*_{pz-pz}) \text{ occupancy})_{2-H} \quad (3)$$

Although ligands such as  $NH_3$  and  $BH_3^{2-}$  are not expected to participate in a significant hyperconjugative interaction with metal  $d_\pi$  orbitals, they are found to have strongly negative ( $-0.054$ ) and positive ( $0.072$ )  $\pi_X$  values, respectively. These ligands carry net charge, relative to the monoanionic ligands (most notably compared with the isoelectronic methyl anion); based on simple electrostatics, the difference in charge would be expected to influence the extent of Ir-to-CO  $\pi$ -donation. The additional negative charge on  $BH_3^{2-}$  (relative to  $CH_3^-$ ) will increase Ir-to-CO  $\pi$ -donation relative to  $CH_3^-$  by polarization of the electronic distribution around the Ir atom in the direction of CO; conversely, relative to  $CH_3^-$ , Ir-to-CO  $\pi$ -donation is reduced by polarization toward neutral  $NH_3$ . These ligands are therefore *effectively* acting as a  $\pi$ -donor and a  $\pi$ -acceptor, respectively, even if they do not significantly donate or accept any  $\pi$ -electron density to or from the Ir center.

The  $\sigma_X$  and  $\pi_X$  parameters of the various ligands are illustrated graphically in Figure 2.

**Oxidative Addition of  $CH_4$  to Three-Coordinate  $trans-(PH_3)_2IrX$ .** The reaction energies for oxidative addition of

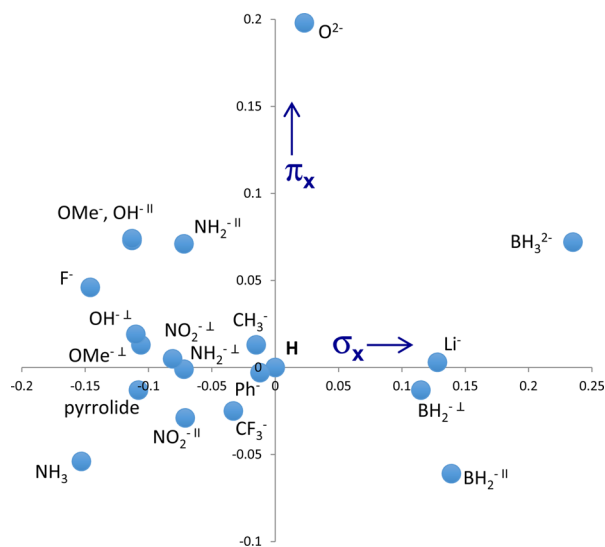


**Figure 2.** Calculated electronic substituent parameters ( $\sigma_X$ ,  $\pi_X$ ) ( $\parallel$  = coplanar with P–Ir–P axis;  $\perp$  = orthogonal to P–Ir–P axis; see Table 1 caption for details).

methane to  $trans-(PH_3)_2IrX$  were calculated for the set of X ligands described in Table 1 ( $\Delta E_X$ , Table 2).<sup>74</sup> Structures for

**Table 2.** Calculated Reaction Energies ( $\Delta E_X$ , kcal/mol) for  $CH_4$  Addition to  $trans-(PH_3)_2IrX$ ; Constrained Geometries Imposed for Three Configurations (see Figure 3 and text)<sup>a</sup>

X ligand	$\Delta E_X$ (kcal/mol)		
	$Y_{Me}$	$Y_X$	$T_H$
$BH_2^-, \perp$	<b>3.8</b>	14.8	15.2
$BH_2^-, \parallel$	<b>-2.0</b>	32.6	18.6
$BH_3^{2-}$	<b>0.3</b>	9.3	15.9
$CF_3^-$	<b>-3.4</b>	3.9	-2.5
$CH_3^-$	<b>-4.9</b>	-4.6	-1.3
$F^-$	-15.1	<b>-35.1</b>	-28.8
$H^-$	<b>-6.9</b>	1.7	-0.7
$Li^-$	<b>-5.4</b>	14.6	15.0
$NH_2^-, \perp^b$	-6.3	<b>-10.4</b>	-8.5
$NH_2^-, \parallel^c$	-10.2	<b>-24.6</b>	-14.4
$NH_3$	-16.1	-28.9	<b>-32.7</b>
$NO_2^-, \perp$	-3.6	-6.6	<b>-10.9</b>
$NO_2^-, \parallel$	-2.4	-0.5	<b>-6.5</b>
$O^{2-}$	0.3	<b>-23.1</b>	-7.5
$OH^-, \perp$	-12.2	<b>-22.8</b>	-18.4
$OH^-, \parallel$	-10.2	<b>-30.6</b>	-20.9
$OMe^-, \perp$	-9.3	<b>-19.4</b>	-15.8
$OMe^-, \parallel$	-9.0	<b>-28.4</b>	-20.2
$Ph^-, \perp$	<b>-1.6</b>	2.9	1.6
pyrrolide, $\perp$	-9.0	-14.7	<b>-16.3</b>

<sup>a</sup> $\parallel$  = coplanar with P–Ir–P axis;  $\perp$  = orthogonal to P–Ir–P axis. For each ligand X, the lowest calculated  $\Delta E_X$  is shown in bold font. <sup>b</sup>H–N–Ir–P dihedral angles set to  $58.5^\circ$ . <sup>c</sup>H–N–Ir–P dihedral angles set to  $31.5^\circ$ .

the three-coordinate reactants and the five-coordinate products were optimized both with and without imposed geometry restrictions. In the restricted geometries, the cis ligand–metal–ligand angles were fixed at  $90^\circ$ . Unless noted otherwise, the Ir–C–H angles of the methyl group of the five-coordinate products were set to tetrahedral values ( $109.47^\circ$ ); selected X ligands (e.g.,  $BH_2^-$ ,  $NO_2^-$ ) were constrained to be coplanar with or orthogonal to the P–Ir–P axis; the P–Ir–P angles were fixed at  $180^\circ$ ; and the remaining ligands were held in the plane perpendicular to the P–Ir–P axis.

We found that the unconstrained geometries of the five-coordinate products (3, formally Ir(III) with a  $d^6$  electronic configuration) fell into three general categories: square pyramidal (SQP, with hydride apical) and two types of distorted trigonal bipyramidal (TBP); this phenomenon has been reported and deeply investigated by Eisenstein.<sup>75–77</sup> These geometries were then grouped according to the three idealized geometries which they closely approximated. Relative to the plane of the  $XIrH(CH_3)$  unit, these geometries are described as (see Figure 3) T-shape (SQP,  $\angle X-Ir-H = 90^\circ$ ,  $\angle X-Ir-Me = 180^\circ$ ; 3- $T_H$ ),  $Y_X$ -shape (distorted TBP,  $\angle Me-Ir-H = 72^\circ$ ,  $\angle X-Ir-H = 144^\circ$ ; 3- $Y_X$ ), and  $Y_{Me}$ -shape (distorted TBP,  $\angle X-Ir-H = 72^\circ$ ,  $\angle Me-Ir-H = 144^\circ$ ; 3- $Y_{Me}$ ). Regression analyses of the correlation of reaction energies with  $\sigma_X$  and  $\pi_X$  parameters showed slightly better numerical fits when the constrained geometries for 3 were used, but

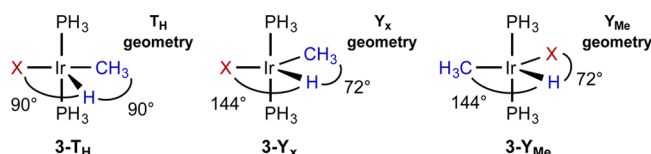


**Figure 3.** Idealized geometries approximating the three energy minima found for five-coordinate species  $trans\text{-}(\text{PH}_3)_2\text{Ir}(\text{X})(\text{H})(\text{CH}_3)$ .

qualitatively, both sets of geometries and regression analyses yield the same conclusions. The variations in geometry among the complexes, however, do introduce some perturbations to the calculated reaction energies that do not straightforwardly result from the underlying electronic factors of the X ligands. Since the overall conclusions remain the same regardless of whether geometry restrictions are imposed or not, only the data referring to constrained geometries are presented below. Analogous data for the complexes with unconstrained geometries are available in the [Supporting Information](#).

Linear regression analysis was performed in which the electronic parameters  $\sigma_X$  and  $\pi_X$  (and the energy value at the origin) were simultaneously fit to the data set comprising the lowest calculated reaction energy (global minimum) for each X ligand (Table 2, values in bold font). For each ligand X the energy of methane addition to  $trans\text{-}(\text{PH}_3)_2\text{IrX}$  is thus  $(C_\sigma\sigma_X + C_\pi\pi_X + Y)$  kcal/mol. The coefficients obtained in this regression equation (eq 4) reveal and quantify the effects of varying ligand X on the thermodynamics of oxidative addition of methane to  $trans\text{-}(\text{PH}_3)_2\text{IrX}$ . The positive coefficient obtained for the  $\sigma_X$  parameter ( $C_\sigma = +85$ ) indicates that *stronger*  $\sigma$ -donating ligands *disfavor* OA; the negative coefficient found for the  $\pi_X$  parameter ( $C_\pi = -86$ ) indicates that OA is favored by stronger  $\pi$ -donating ligands.

$$\Delta E_X = (85 \pm 15)\sigma_X + (-86 \pm 27)\pi_X + (-10 \pm 2) \quad (4)$$

$$R^2 = 0.72$$

The magnitudes of the respective regression coefficients are not directly comparable, since the  $\sigma_X$  and  $\pi_X$  parameters are

derived from different molecular properties (bond length and orbital occupancy, respectively). However, a quantitative measure of the relative effect of the  $\sigma/\pi$  contributions on the reaction energy was formulated by multiplying the  $\sigma_X$  and  $\pi_X$  parameters of the ligands X (Table 1) by the respective regression coefficients ( $C_\sigma$  and  $C_\pi$ ). For each ligand X the energy of methane addition is  $(C_\sigma\sigma_X + C_\pi\pi_X + Y)$  kcal/mol. The standard deviations (SDs) of the values of  $C_\sigma\sigma_X$  and  $C_\pi\pi_X$  thus serve as a measure of the variability of the thermodynamics attributable to the variability of the  $\sigma$ -donating and  $\pi$ -donating/withdrawing properties, respectively. The identical values are obtained if we take the standard deviations of the  $\sigma_X$  and  $\pi_X$  parameters for the set of ligands used (0.107 and 0.058, respectively) as a measure of the variability of these parameters and multiply those values by the respective regression coefficients.

This analysis indicates (Table 3; top row, global minima) that the unfavorable effect of increased  $\sigma$ -donation by X (SD = 9.1 kcal/mol) is considerably greater than the favorable effect of increased  $\pi$ -donation (SD = 5.0 kcal/mol). This computational result, obtained for the prototypical case of C–H addition to a transition metal complex ( $\text{IrL}_2\text{X}$ ), is strongly discordant with the widely held view that “more electron-donating ligands” favor oxidative addition, even if this model is generally recognized as being a simplification.

This regression analysis is based on selecting the lowest energy conformer from among the three possibilities considered for each ligand X (cf. Figure 3). Thus, this analysis presumably provides the closest approximation to anticipated experimental results. However, this approach may be less suitable for elucidating a fundamental understanding of how ancillary ligand electronic factors directly influence the thermodynamics of OA because the energies of different geometries are expected to respond differently to variations of the electronic parameters.

Sets of conformer-specific regression coefficients, which are probably more meaningful at a fundamental level, were obtained by treating the formation of each conformational

**Table 3.** Regression Equations Using Restricted Geometries for 3- $Y_{\text{Me}}$ , 3- $Y_X$ , and 3- $T_H$ .

reaction / product isomer	regression equation	SD <sup>a</sup> of $\sigma$ effects (kcal/mol)	SD <sup>a</sup> of $\pi$ effects (kcal/mol)
	$\Delta E_X = (85 \pm 15)\sigma_X + (-86 \pm 27)\pi_X + (-10 \pm 2)$	+9.1	-5.0
	$\Delta E_X = (131 \pm 10)\sigma_X + (-48 \pm 18)\pi_X + (-2 \pm 1)$	+14.0	-2.8
	$\Delta E_X = (142 \pm 13)\sigma_X + (-156 \pm 24)\pi_X + (-1 \pm 1)$	+15.2	-9.1
	$\Delta E_X = (37 \pm 8)\sigma_X + (5 \pm 14)\pi_X + (-5 \pm 1)$	+4.0	+0.3

<sup>a</sup>SD = standard deviation. The sign (+ or -) of a particular regression coefficient indicates the direction of the effect: a positive value indicates that increased electron donation disfavors the reaction and hence increases the energy of addition. The signs of the regression coefficients are applied to the SDs to indicate direction of the effects although actual standard deviations are necessarily positive.

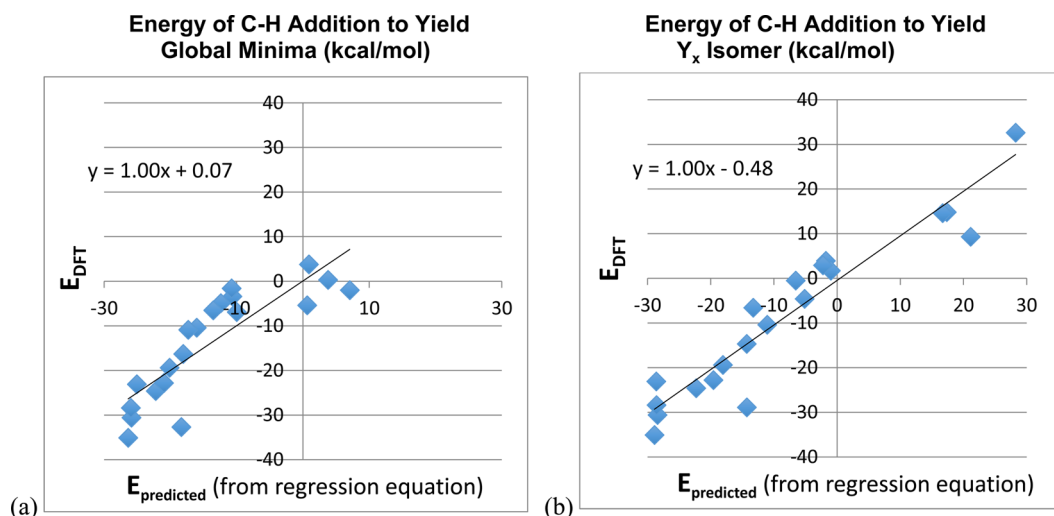


**Figure 4.** (a) Plot of calculated (DFT) reaction energies for methane C–H addition to *trans*-(PH<sub>3</sub>)<sub>2</sub>IrX to give lowest energy isomer vs energies predicted based on the regression equation:  $\Delta E_{X\text{-predicted}} = (85 \pm 15)\sigma_X + (-86 \pm 27)\pi_X + (-10 \pm 2)$  kcal/mol (see Table 3). (b) Plot of calculated (DFT) reaction energies for methane C–H addition to *trans*-(PH<sub>3</sub>)<sub>2</sub>IrX to give the Y<sub>X</sub> isomer vs energies predicted based on the regression equation:  $\Delta E_{X\text{-predicted}} = (142 \pm 13)\sigma_X + (-156 \pm 24)\pi_X + (-1 \pm 1)$  kcal/mol (see Table 3; see Supporting Information for analogous plots for T<sub>H</sub> and Y<sub>Me</sub> isomers, and a note about the corresponding values of R<sup>2</sup>).

**Table 4. Regression Equations Using Restricted Geometries for (a) Addition of Methane to 1 To Give the X-Apical Square Pyramidal Geometry (3-T<sub>X</sub>) and (b) Addition of Methane to *cis*-(PH<sub>3</sub>)<sub>2</sub>IrX To Give 3-T<sub>H/cis</sub>PH<sub>3</sub>**

reaction / product isomer	regression equation	SD <sup>a</sup> of $\sigma$ effects (kcal/mol)	SD <sup>a</sup> of $\pi$ effects (kcal/mol)
	$\Delta E_X = (-38 \pm 7)\sigma_X + (14 \pm 20)\pi_X + (2 \pm 1)$	-4.0	+0.5
	$\Delta E_X = (3 \pm 16)\sigma_X + (28 \pm 26)\pi_X + (-15 \pm 2)$	+0.3	+1.9

<sup>a</sup>SD = standard deviation. The sign (+ or -) of a particular regression coefficient indicates the direction of the effect: a positive value indicates that increased electron donation disfavors the reaction and hence increases the energy of addition.

isomer, Y<sub>Me</sub>, Y<sub>X</sub>, or T<sub>H</sub> (Figure 3), separately; the resulting regression equations with reaction energies from Table 2 are presented in Table 3. For each of these three isomers, C<sub>σ</sub> is significantly positive. These results indicate that *oxidative addition is disfavored by more  $\sigma$ -donating ligands*, independent of product geometry. The coefficient for the  $\pi_X$  parameter varies from a significantly negative value ( $\pi$ -donation favors oxidative addition) in the case of the Y<sub>X</sub> conformer, through an intermediate, modestly negative value for the T<sub>H</sub> conformer, to effectively zero for Y<sub>Me</sub>. A plot giving an indication of the fit of the data to eq 4 (for the global minima) and a representative plot (for Y<sub>X</sub>) illustrating the fit to the other, isomer-specific, equations in Table 3 are found in Figure 4. (Analogous plots for T<sub>H</sub> and Y<sub>Me</sub> are given in Figure S-2. A “3-D” plot of  $\Delta E_X$  vs the individual parameters  $\sigma_X$  and  $\pi_X$ , as opposed to the multivariable terms used in the “2-D” plots of Figure 4 and Figure S-1, is given in Figure S-1.)

For all three conformational isomers we find that the unfavorable effect of increased  $\sigma$ -donation on the reaction energy is much greater than any favorable effect of increased  $\pi$ -donation. For 3-T<sub>H</sub> and 3-Y<sub>Me</sub>, the variability due to  $\sigma$  effects is indicated by SDs of 14.0 and 4.0 kcal/mol, respectively. The variability due to  $\pi$  effects gives SDs of only 2.8 and 0.3 kcal/mol, respectively. For 3-Y<sub>X</sub>, the SD of  $\sigma$  effects (15.2 kcal/mol)

remains considerably greater than the SD of  $\pi$  effects (9.1 kcal/mol), but the significantly favorable effect of  $\pi$ -donation by X for this conformer is noteworthy.<sup>75–77</sup>

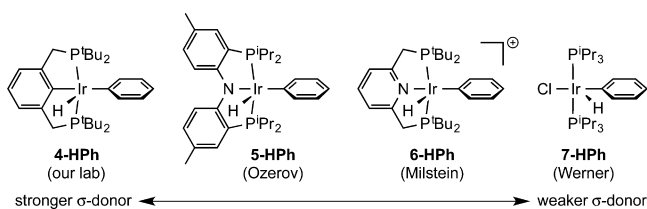
In the very few cases in which the X ligand exerts a stronger trans-influence than hydride or methyl,<sup>38,77,78</sup> the five-coordinate complex may adopt a square pyramidal geometry in which X is found in the apical position (3-T<sub>X</sub>). In the regression equation for this geometry (using the set of parameters and X ligands from Table 2), a reversal of preference for  $\sigma$  effects is observed (Table 4); the  $\sigma_X$  parameter coefficient is slightly negative, i.e., a stronger  $\sigma$ -donating ligand slightly favors oxidative addition. However, the ( $\sigma_X$ ,  $\pi_X$ ) regression coefficients are both small, indicating a limited magnitude of the substituent effects of X for this conformational isomer.

In the systems discussed to this point, the variable ligand X has been positioned trans to the site of C–H addition. We have also explored the effects of varying the ligand cis to the site of addition by calculating the energy of methane OA to *cis*-(PH<sub>3</sub>)<sub>2</sub>IrX complexes, using the same set of X ligands listed in Table 1. The five-coordinate structures were restricted to an SQP geometry with the hydride located in the apical position (3-T<sub>H-cis</sub>PH<sub>3</sub>), and a multivariable linear regression was performed analogously to the treatment for the *trans*-

(PH<sub>3</sub>)<sub>2</sub>IrX complexes described above. The  $\sigma_X$  parameter coefficient was found to be essentially zero while the  $\pi_X$  parameter coefficient was small and positive ( $C_\pi = 28$ ) with a standard error (26) approximately equal to the coefficient itself. Thus the calculations indicate that the nature of X (among the set of X ligands studied) has little effect on the thermodynamics of C–H addition to *cis*-(PH<sub>3</sub>)<sub>2</sub>IrX.

**Experimental Results.** The calculations described above involve model complexes for which it is unfortunately not possible to experimentally test any of the calculated values. However, the principal conclusions, namely that C–H addition is disfavored by  $\sigma$ -donating coordinating groups positioned trans to the coordination site of addition and, to a lesser extent, favored by  $\pi$ -donating groups, are amenable to experimental verification. A series of isoelectronic, five-coordinate Ir(III) phenyl hydride complexes previously reported may serve as a suitable set of complexes to test our computation-based conclusions (Scheme 2): (PCP)Ir(H)(Ph) (**4-HPh**) (PCP =

### Scheme 2. Ir(III) Phenyl Hydride Complexes Investigated Experimentally<sup>a</sup>



<sup>a</sup>Relative  $\sigma$ -donating abilities of the pincer central coordinating group are indicated.

$\kappa^3$ -C<sub>6</sub>H<sub>3</sub>-2,6-(CH<sub>2</sub>P<sup>t</sup>Bu<sub>2</sub>)<sub>2</sub>), synthesized in one of our laboratories;<sup>79</sup> (AmPnP)Ir(H)(Ph) (**5-HPh**) (AmPnP =  $\kappa^3$ -bis(2-diisopropylphosphino-4-methylphenyl)amide), reported by Ozerov;<sup>80</sup> (PyPnP)Ir(H)(Ph)<sup>+</sup>PF<sub>6</sub><sup>-</sup> (**6-HPh**) (PyPnP =  $\kappa^3$ -C<sub>5</sub>H<sub>3</sub>N-2,6-(CH<sub>2</sub>P<sup>t</sup>Bu<sub>2</sub>)<sub>2</sub>), reported by Milstein,<sup>81,82</sup> and *trans*-(P<sup>t</sup>Pr<sub>3</sub>)<sub>2</sub>Ir(Cl)(H)(Ph) (**7-HPh**), reported by Werner.<sup>83,84</sup> This series of three-coordinate complexes (4–7) features central coordinating groups with widely varying  $\sigma$ -donating abilities. Thus, complex 4 bears a strongly  $\sigma$ -donating aryl carbon, while complex 7 has a weakly  $\sigma$ -donating chloride. Complexes 5 and 6 feature an amido and a pyridyl nitrogen, respectively, which are expected to have  $\sigma$ -donating abilities intermediate between the central groups of the ligands featured in 4 and 7.

The ( $\sigma_X$ ,  $\pi_X$ ) parameter values for the pincer ligands in three-coordinate complexes 4–7 were derived from calculations on the corresponding four-coordinate ammonia and carbonyl complexes (Table 5). The values thus determined were found

**Table 5. Calculated  $\sigma_X$  and  $\pi_X$  Parameters for Complexes 4–7, Energies of Reductive Elimination of Methane from 4-HMe–7-HMe Predicted Based on  $\sigma_X$  and  $\pi_X$  Parameters, and Energies and Enthalpies Calculated Using DFT<sup>a</sup>**

M(H)(Me)	M(H)(Me) → M + CH <sub>4</sub>				
	$\sigma_X$	$\pi_X$	$\Delta E_{\text{RE-regression}}$	$\Delta E_{\text{RE-DFT}}$	$\Delta H_{\text{RE-DFT}}$
4-HMe	−0.015	−0.004	3.0	2.1	2.4
5-HMe	−0.129	0.024	23.5	28.6	28.7
6-HMe	−0.139	−0.037	15.4	23.6	23.7
7-HMe	−0.169	0.035	31.0	35.4	35.1

<sup>a</sup>Units for  $\Delta E$  and  $\Delta H$  are kcal/mol.

to be approximately consistent with their closest (PH<sub>3</sub>)<sub>2</sub>IrX model analogues (Table 1). The  $\sigma_X$  parameter for the pincer ligand of 4 is close to zero, whereas the  $\sigma_X$  values for complexes 5–7 are significantly negative, indicating weak  $\sigma$ -donation by the central coordinating groups. The  $\pi_X$  parameter values obtained indicate that the ligands in complexes 5 and 7 are moderate  $\pi$ -donors, whereas the pincer ligand of cationic complex 6 acts as a moderate  $\pi$ -acceptor; the phenyl donor in the pincer ligand of complex 4 is neither a significant  $\pi$ -donor nor a significant  $\pi$ -acceptor.

Using the  $\sigma_X$  and  $\pi_X$  parameter values thus obtained (Table 5), the reaction energies for the oxidative addition of methane ( $\Delta E_{\text{OA}}$ ) were predicted using the regression equation derived for the Y<sub>X</sub> geometry (Table 3); the predicted energies of the microscopically reverse reaction, reductive elimination ( $\Delta E_{\text{RE}} = -\Delta E_{\text{OA}}$ ), are presented as  $\Delta E_{\text{RE-regression}}$  in Table 5. The  $\Delta E_{\text{RE-regression}}$  values increase with increasingly negative values of the  $\sigma_X$  parameter, except when the two PNP-pincer complexes 5-HMe and 6-HMe are compared directly. The amido ligand of complex 5 ( $\pi_X = 0.024$ ) is calculated to be a much stronger  $\pi$ -donor than the pyridine-based ligand of complex 6 ( $\pi_X = -0.037$ ); this large difference in  $\pi$ -donating ability overrides the modest difference in  $\sigma$ -donation. Thus the reductive elimination of methane from amido-ligated 5-HMe is predicted (23.5 kcal/mol) to be more endoergic than elimination from pyridine-ligated 6-HMe (15.4 kcal/mol). DFT electronic structure calculations (see Computational Methods) for the energies of methane reductive elimination afford results ( $\Delta E_{\text{RE-DFT}}$ : 4-HMe  $\ll$  6-HMe < 5-HMe < 7-HMe; Table 5) consistent with the trend derived from the values predicted based on the regression equation ( $\Delta E_{\text{RE-regression}}$ ).

Values of  $\Delta E_{\text{RE-DFT}}$  for elimination of benzene across the series of complexes 4-HPh to 7-HPh (Table 6) follow the same

**Table 6. Calculated Energies and Enthalpies of Benzene Reductive Elimination and Reductive Coupling ( $\sigma$ -Complex Formation) for Complexes 4-HPh–7-HPh<sup>a</sup>**

M(H)(Ph)	M(H)(Ph) → M( $\sigma$ -HPh)			M(H)(Ph) → M + PhH	
	$\Delta E_{\text{RC-DFT}}^\ddagger$	$\Delta H_{\text{RC-DFT}}^\ddagger$	$\Delta G_{\text{RC-DFT}}^\ddagger$	$\Delta E_{\text{RE-DFT}}$	$\Delta H_{\text{RE-DFT}}$
4-HPh	14.1	13.9	<b>14.8</b>	11.7	11.9
5-HPh	29.2	28.5	28.4	37.9	<b>38.4</b>
6-HPh	16.8	16.4	17.3	30.8	<b>31.1</b>
7-HPh	33.3	32.1	31.9	42.1	<b>41.7</b>

<sup>a</sup>See text and Figure 5 for elaboration of the distinction between reductive coupling (RC) and reductive elimination (RE). Units for  $\Delta E$ ,  $\Delta H$ , and  $\Delta G$  are kcal/mol. Standard state for  $\Delta G$  is  $T = 298.15$  K and  $P = 1$  atm for each species participating in the reaction. Values in bold are the best estimates for  $\Delta G^\ddagger$  for reductive elimination, calculated directly in the case of 4-HPh and approximated as  $\Delta H_{\text{RE-DFT}}$  for 5-HPh, 6-HPh, and 7-HPh; cf. text. Values in italics for 5-HPh are best estimates; see ref 85 for details.

order as those for methane, but they are uniformly 7–10 kcal/mol greater (cf. Table 5). Direct experimental determination of the thermodynamics of phenyl hydride reductive elimination is not possible as the three-coordinate complexes 4–7 have not been observed; however, the kinetics of reductive elimination can be measured. Our computational DFT results indicate that, for complex 4-HPh, the TS for reductive coupling (C–H bond formation) directly leads to the loss of benzene, i.e. reductive elimination. This transition state, TS(RC), which corresponds



to a calculated barrier  $\Delta H_{RC-DFT}^{\ddagger} = \Delta H_{RE-DFT}^{\ddagger} = 13.9$  kcal/mol and  $\Delta G_{RC-DFT}^{\ddagger} = \Delta G_{RE-DFT}^{\ddagger} = 14.8$  kcal/mol (Table 6), is 2 kcal/mol higher in enthalpy than the free three-coordinate complex plus free benzene (Figure 5a). In contrast, for

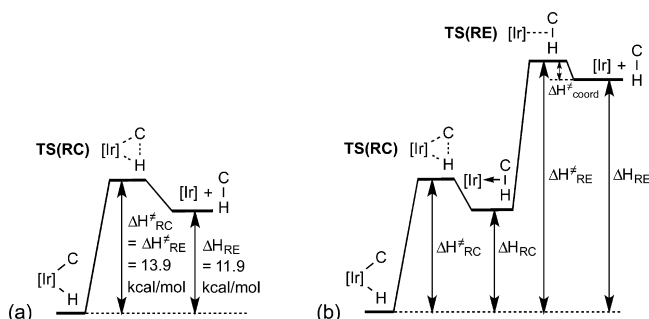


**Figure 5.** Schematic enthalpy diagrams for C–H reductive elimination from (a) 4-HPh and (b) complexes 5-HPh, 6-HPh, and 7-HPh. ([Ir] is the respective three-coordinate species. C–H = Ph–H.) The enthalpy of the reductive coupling transition state, TS(RC), is calculated to be significantly lower than that of the free species, [Ir] plus C–H for reactions of 5-HPh, 6-HPh, and 7-HPh.

complexes 5-HPh, 6-HPh, and 7-HPh, the transition states for reductive coupling, TS(RC) (Figure 5b), lead to  $\sigma$ (C–H)-bound species with enthalpies that are well below the enthalpies of the respective free species.

We were unable to locate conventional transition states for the dissociation of these  $\sigma$ -C–H complexes (TS(RE)), the TS for the overall reductive elimination reaction). However, the reverse step, C–H bond coordination of benzene to the three-coordinate Ir(I) complexes 5–7, is expected to be a barrierless or a nearly barrierless process ( $\Delta H_{coord}^{\ddagger}$  is expected to be nearly zero). In that case,  $\Delta H_{RE}^{\ddagger}$  for the reductive elimination of benzene from complexes 5-HPh, 6-HPh, and 7-HPh would be approximately equal to the thermodynamic value,  $\Delta H_{RE}$  (Table 6;  $\Delta S_{RE}$  is clearly very positive due to formation of free benzene, but we expect  $\Delta S_{RE}^{\ddagger}$  to be of much smaller magnitude).

We thus assume that, to a rough approximation,  $\Delta H_{RE}^{\ddagger} = \Delta H_{RE}$  (see Figure 5a and 5b), and hence the RE/OA thermodynamics may be elucidated, experimentally, from measurements of the RE kinetics. Toward this end, EXSY NMR experiments were performed with complex 4-HPh at a range of temperatures from  $-54$  to  $-27$  °C. (We have previously shown that arene/arene exchange proceeds via a dissociative process.<sup>79</sup>) An Eyring plot yielded activation parameters for reductive elimination of  $\Delta H_{RE}^{\ddagger} = 13.2$  kcal/mol and  $\Delta S_{RE}^{\ddagger} = -2$  eu (Table 7), in excellent agreement with the computed values ( $\Delta H_{RE-DFT}^{\ddagger} = 13.9$  kcal/mol,  $\Delta S_{RE-DFT}^{\ddagger} = -3$  eu at 25 °C; Table 6). The rate of reductive elimination from amido-PNP complex 5-HPh was measured at a range of temperatures from 85 to 114 °C by monitoring the rate of disappearance of the hydride signal upon exchange with toluene- $d_8$ . The enthalpic and entropic contributions to the barrier were determined to be  $\Delta H_{RE}^{\ddagger} = 31.2$  kcal/mol and  $\Delta S_{RE}^{\ddagger} = 6$  eu (consistent with a dissociative mechanism), respectively; thus, at 25 °C,  $\Delta G_{RE}^{\ddagger} = 29.4$  kcal/mol which is much greater than the corresponding value for 4-HPh ( $\Delta G_{RE}^{\ddagger} = 13.8$  kcal/mol). The rate of reductive elimination for pyridine-based PNP complex 6-HPh at 84 °C was determined to be  $1.3 \times 10^{-4}$  s $^{-1}$ , which corresponds to a kinetic barrier  $\Delta G_{RE}^{\ddagger} = 27.4$  kcal/mol. For chloride complex 7-HPh, a

**Table 7.** Experimentally Determined Kinetic Parameters for the Reductive Elimination of Benzene from Complexes 4-HPh–7-HPh<sup>a</sup>

M(H)(Ph)	M(H)(Ph) → M + HPh			
	$\Delta H_{RE}^{\ddagger}$	$\Delta S_{RE}^{\ddagger}$	$\Delta G_{RE}^{\ddagger}$ (T = 84 °C)	$\Delta G_{RE}^{\ddagger}$ (T = 120 °C)
4-HPh	13.2 (±0.9)	-2 (±4)	13.8 <sup>b</sup>	13.9 <sup>b</sup>
5-HPh	31.2 (±1.9)	6 (±5)	29.0 <sup>b</sup>	28.7 <sup>b</sup>
6-HPh	$k = 1.25 \times 10^{-4}$ s $^{-1}$ (at 84 °C)		27.4	27.5 <sup>b,c</sup>
7-HPh	$k \leq 5.0 \times 10^{-5}$ s $^{-1}$ (at 120 °C)		$\geq 31.2^{b,d}$	$\geq 30.9$

<sup>a</sup>Units for  $\Delta H_{RE}^{\ddagger}$  and  $\Delta G_{RE}^{\ddagger}$  are kcal/mol; units for  $\Delta S_{RE}^{\ddagger}$  are eu. <sup>b</sup>Extrapolated values. <sup>c</sup>Calculated with  $\Delta S_{RE}^{\ddagger} = -2$  eu. <sup>d</sup>Calculated with  $\Delta S_{RE}^{\ddagger} = 6$  eu.

conservative upper limit for the rate of benzene dissociation at 120 °C was previously reported to be  $5 \times 10^{-5}$  s $^{-1}$ , corresponding to a kinetic barrier  $\Delta G_{RE}^{\ddagger} \geq 30.9$  kcal/mol.<sup>84</sup>

The trend for the relative experimental rates of benzene C–H reductive elimination (Table 7) correlates well with the trend from DFT calculations (Table 6) and, more significantly, conforms well with the general conclusions drawn from our studies of (methane) C–H addition to model *trans*-Ir(PH<sub>3</sub>)<sub>2</sub>X complexes presented above. The barrier to reductive elimination from complex 4-HPh, bearing the strongly  $\sigma$ -donating aryl ligand, was found to be the smallest, by a substantial margin (presumably reflecting the least endoergic C–H reductive elimination), while that for reductive elimination from complex 7-HPh, bearing the most weakly  $\sigma$ -donating central coordinating group (chloride), was found to be the largest. The magnitudes of the barriers for elimination from complexes 5-HPh and 6-HPh, which have ligands of intermediate  $\sigma$ -donating ability, were in between those of 4-HPh and 7-HPh. The amido group of the anionic ligand in 5 is a stronger  $\sigma$ -donor than a pyridine; however, the amido group is also a much stronger  $\pi$ -donor than a pyridine. Accordingly, the rates of C–H elimination from these two N-coordinated pincer complexes are similar, with only a slightly greater barrier measured for elimination from the amido complex 5-HPh compared with pyridine-based 6-HPh (Table 7). Finally we note that the comparison among these complexes cannot be considered quantitative, since steric factors are not constant throughout the set of pincer ligands. Complexes 4-HPh and 6-HPh, however, are isosteric and isoelectronic (the only difference being a neutral pyridine N atom rather than an anionic phenyl carbon bound to the Ir center). Thus the much slower rate of elimination from PNP complex 6-HPh vs PCP complex 4-HPh affords particularly strong support for the conclusion of more favorable thermodynamics of OA to a complex with a more weakly  $\sigma$ -donating central coordinating group, X.

Finally we note that Turculet has reported<sup>86</sup> a PSiP-pincer iridium phenyl hydride complex (8-HPh), which is sterically similar to amido-PNP complex 5-HPh. 8-PhH was reported to be cleanly converted to the corresponding C<sub>6</sub>D<sub>6</sub> adduct after 14 h at room temperature (Figure 6). Assuming that this period thus corresponds to at least 4 half-lives for elimination, the upper limit of  $\Delta G_{RE}^{\ddagger}$  for this exchange reaction (at ca. 21 °C) is ca. 22.9 kcal/mol as compared with 29.4 kcal/mol for 5-HPh (extrapolated to 21 °C). Although we have only parametrized X ligands with metal-bound second-row atoms, silyl groups are well-known to exert a strong trans-influence.<sup>87–89</sup> Thus the



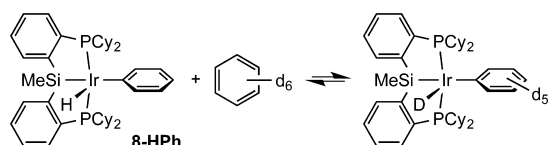


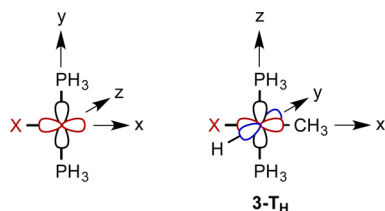
**Figure 6.** Exchange reaction of Turculet's PSiP complex **8-HPh** with  $C_6D_6$  (ref 86).

much lower barrier to C–H elimination from **8-PhH** as compared with **5-PhH** (or from **6-PhH** or **7-PhH**) offers further support and some generalization of our conclusions.

**An Orbital-Based Rationale.** The conclusions reached above regarding the effects of varying ancillary ligand  $\sigma/\pi$ -donation on OA thermodynamics may be rationalized based on consideration of orbital interactions in the three-coordinate  $d^8$  Ir(I) reactant and the five-coordinate  $d^6$  Ir(III) product complexes. Our results are most conveniently rationalized using Landis's representation of  $sd^n$ -hybridized metal orbitals.<sup>90–92</sup>

In the three-coordinate  $trans-(PH_3)_2IrX$  complexes, the  $d^8$  Ir(I) atom can be viewed as having doubly occupied  $5d_{xy}$ ,  $5d_{xz}$ ,  $5d_{yz}$ , and  $5d_z^2$  orbitals (the  $z$  axis is perpendicular to the plane containing the P, X, and Ir atoms, **Scheme 3**); thus, the

**Scheme 3.** Illustration of Unoccupied  $sd$  Hybrid Orbitals and Coordinate Scheme Applied for  $trans-(PH_3)_2IrX$  and **3-T<sub>H</sub>**



phosphine and X ligands are donating into two empty  $sd$  hybrid orbitals, derived from the  $5d_{x^2-y^2}$  orbital (oriented along the P–Ir–P ( $y$ ) and the X–Ir ( $x$ ) axes) and the  $6s$  orbital, as shown in **Scheme 3**. In the five-coordinate  $d^6$  Ir(III) complexes, the  $5d_z^2$  orbital has been formally vacated, and three  $sd^2$ -hybridized orbitals now arise from combination of the iridium  $5d_{x^2-y^2}$ ,  $5d_z^2$ , and  $6s$  orbitals. For all the isomeric five-coordinate complexes, one of these  $sd^2$ -hybridized orbitals is oriented along the P–Ir–P axis, while the remaining two hybrids are positioned in the

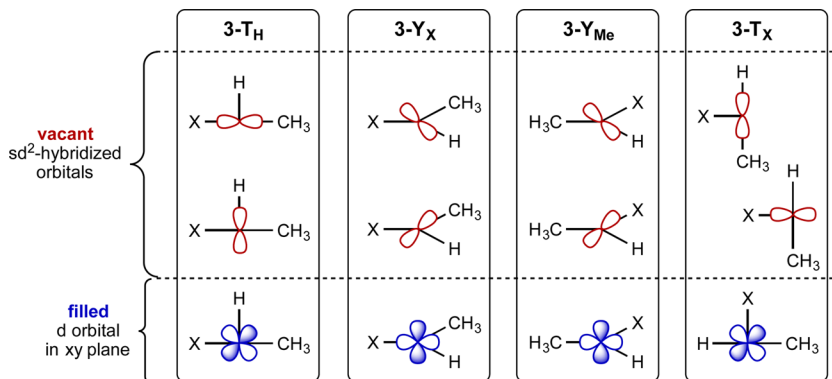
plane perpendicular to the P–Ir–P axis (note that the axes are now defined such that this is the  $xy$  plane).

**$\sigma$ -Type Interactions.** Of the isomeric five-coordinate adducts, we first consider the square pyramidal **3-T<sub>H</sub>** geometry for which the vacant  $sd^2$ -hybridized orbitals are oriented along the Ir–X, Ir–P, and Ir–H axes (**Scheme 4**; only orbitals in the  $xy$  plane are shown). If we limit our examination of  $\sigma$ -type interactions to the plane containing X, Ir, H, and Me (the  $xy$  or “equatorial” plane), then the orbital picture can be simplified to contain just three orbitals: a filled  $d_{xy}$  orbital and two empty  $sd^2$ -hybridized orbitals; the latter, when considered together, resemble the  $d_{x^2-y^2}$  orbital (**Scheme 4**). The X, Me, and H groups of **3-T<sub>H</sub>** interact directly with these two empty  $sd^2$ -hybridized orbitals. The very strong trans-influence hydride is the lone ligand donating into the  $sd^2$  orbital oriented along the  $y$  axis. The X ligand must “share” one of the  $sd^2$  orbitals with the Me group trans to it (a 3c–4e interaction), in contrast with the situation in three-coordinate  $trans-(PH_3)_2IrX$  species. Hence, a more  $\sigma$ -donating ligand X will more strongly disfavor additional donation from what is formally a methyl anion into the same  $sd^n$  orbital. A more strongly  $\sigma$ -donating X ligand, however, will also favor vacating the  $d_z^2$  orbital of  $trans-(PH_3)_2IrX$ , which will favor the energetics of OA, but this effect is expected to be relatively small because the donor  $\sigma$ -orbital of X is overlapping with only the torus of the  $d_z^2$  orbital.

Now considering the **Y<sub>X</sub>** geometry (**Scheme 4**), the Me and H groups, both strong trans-influence ligands, each interact strongly with one of the two empty  $sd^2$ -hybrid orbitals. The  $\sigma$  orbital of the X ligand must then donate into the doubly occupied  $d$  orbital in the  $xy$  plane; the energetic penalty of this interaction is increased by the increased  $\sigma$ -donating ability of X, in particular when this is considered relative to  $\sigma$ -donation into an empty  $sd$  orbital as in  $trans-(PH_3)_2IrX$ .<sup>75–77</sup>

In the **Y<sub>Me</sub>** geometry, Me and X switch places relative to the **Y<sub>X</sub>** geometry (**Scheme 4**). The  $\sigma$  orbital of the X ligand is now oriented to interact primarily with an empty  $sd^2$ -hybridized orbital; accordingly, the regression analysis indicates a much smaller (ca. 25%, cf. **Table 3**) unfavorable effect of increased  $\sigma$ -donation than found for the **Y<sub>X</sub>** and **T<sub>H</sub>** geometries. The residual effect that is obtained may arise because of either or both of the following factors: (i) the overlap of the  $\sigma$ -orbital of X with the Ir  $sd^2$ -orbital is slightly reduced (relative to  $trans-(PH_3)_2IrX$ ) as X is positioned ca.  $9^\circ$  off the axis, and (ii) the Me group engages in an unfavorable (albeit small) interaction with the same  $sd^2$  orbital.

**Scheme 4.** Orientation of Filled  $d$  and Vacant  $sd^2$ -hybridized Orbitals in the  $xy$  Plane of **3-T<sub>H</sub>**, **3-Y<sub>X</sub>**, **3-Y<sub>Me</sub>**, and **3-T<sub>X</sub>**<sup>a</sup>



<sup>a</sup>For detailed discussion of the nature of  $sd^n$  hybrid orbitals, see ref 91.

Finally, for the 3- $T_X$  geometry (which is not the global minimum for any of the investigated X ligands) the regression equation indicates that  $\sigma$ -donating ligands slightly favor oxidative addition. In this putative product geometry, the  $\sigma$  orbital of the X ligand is not forced to “share” an  $sd^2$ -hybridized orbital with another ligand, just as it does not in *trans*-( $PH_3$ )<sub>2</sub>IrX. The slight favorability of greater  $\sigma$ -donation presumably arises, at least in part, from the antibonding interaction of X with the torus of the filled  $5d_{z^2}$  orbital of *trans*-( $PH_3$ )<sub>2</sub>IrX, but it is important to note that this effect is relatively small.

**$\pi$ -Type Interactions.** The effect of varying the degree of  $\pi$ -donation or  $\pi$ -withdrawal by X, as indicated by the regression analyses, is also consistent with the proposed orbital interactions. In the three-coordinate *trans*-( $PH_3$ )<sub>2</sub>IrX complexes, the  $\pi$ -type atomic or molecular orbitals of X would interact with the corresponding filled off-axis d orbitals ( $5d_{xy}$  and  $5d_{xz}$ ). In the five-coordinate  $d^6$  Ir(III) complexes, the  $\pi$  interactions are more complex.

Considering the equatorial plane for the 3- $Y_X$  geometry, the major X–metal  $\pi$  interactions involve the empty  $sd^2$ -hybridized orbitals (Scheme 4) so that oxidative addition to afford the 3- $Y_X$  geometry becomes strongly favored by  $\pi$  donation from X; consequently, the  $\pi_X$  coefficient from the 3- $Y_X$  regression equation is negative and with a much larger absolute value than that obtained for any other geometry (Table 3). This effect has been particularly well elaborated by Eisenstein and co-workers.<sup>75–77</sup>

For the 3- $T_H$  geometry, the X–Ir  $\pi$  interactions are approximately the same as those in the three-coordinate complexes and involve overlap with two filled  $d_\pi$  orbitals (the one located in the  $xy$  plane and the other, not shown in Scheme 4, in the  $yz$  plane) suggesting little to no effect on the energetics of OA from the  $\pi$ -donating ability of X. Indeed, the  $\pi_X$  coefficient of the 3- $T_H$  regression equation is small ( $C_\pi = -48$ ; SD =  $-2.8$  kcal/mol), but it is non-negligible, indicating that OA is slightly favored by increased  $\pi$  donation. This may be attributable to the interaction of an X  $\pi$ -symmetry orbital (atomic or molecular) with the empty  $sd^2$  hybrid orbital oriented along the  $y$  axis (which is polarized by interaction with the hydride ligand).

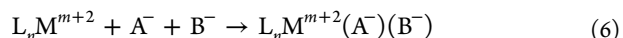
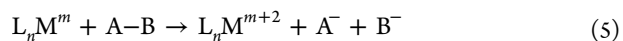
The  $T_X$  geometry differs from  $T_H$  in that the Me group is now trans to H instead of X. The regression equation for this isomer suggests little or no  $\pi$ -effect on the thermodynamics of OA, with a  $\pi_X$  coefficient that is effectively zero ( $C_\pi = 14 \pm 20$ , Table 4). In this case the  $sd^2$  hybrid orbital oriented along the  $y$  axis interacts with both H and Me. This raises its energy relative to the analogous orbital in  $T_H$  and engenders greater (non- $\pi$ ) symmetry; both effects would reduce the importance of  $\pi$ -interactions with X.

In the 3- $Y_{Me}$  geometry, the  $\pi$ -type interactions would be approximately the same as those in the three-coordinate complexes. Accordingly, the computed  $\pi_X$  coefficient is zero within the error of the regression ( $C_\pi = 5 \pm 14$ , Table 3), implying that  $\pi$  effects have little or no influence on the energy of OA to give this geometry.

#### The Orbital-Based Rationale: A General Perspective.

The essence of the explanations offered above can be stated as follows. The oxidative addition reaction may be considered, particularly for the purposes of a thermodynamic cycle, as a composite of (a) the transfer of two electrons from the metal to substrate A–B, inducing cleavage of the A–B bond and formation of reduced fragments  $A^-$  and  $B^-$  (eq 5), and (b)

coordination of  $A^-$  and  $B^-$  to the oxidized metal fragment (eq 6).

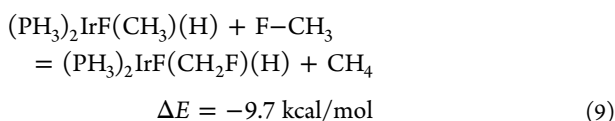
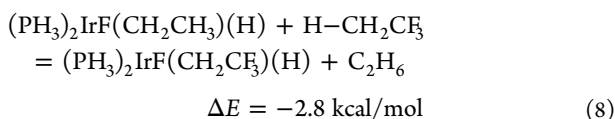
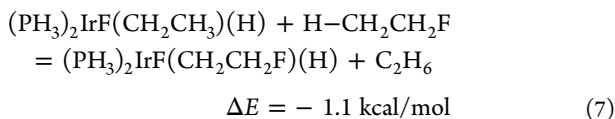


The overall transfer of electron density from the metal center in eqs 5 and 6 must be quite small because the bonds formed are largely covalent. However, the addition or removal of electron density to or from the metal valence orbitals is not uniform. In the systems studied in this work (and probably in most OA reactions), electron density is not removed (eq 5) from metal orbitals that possess  $\sigma$ -symmetry with respect to the ancillary ligands; such orbitals are antibonding and therefore typically unoccupied prior to OA. Depending on the electronic configuration of the metal atom, the electron density may well be removed from a filled metal-based orbital of  $\pi$ -symmetry. In this case, the oxidative addition would be rendered slightly more favorable by greater  $\pi$ -donation of the ancillary ligands. Coordination of  $A^-$  and  $B^-$  (eq 6) then returns to the metal all or most of the electron density lost from the metal in eq 5. This electron density is generally returned, through addition of  $A^-$  and  $B^-$ , into metal-based orbitals that possess  $\sigma$ -symmetry with respect to the ancillary ligands via the formation of 3c-2e bonds. This is expected to be strongly disfavored by increasing  $\sigma$ -donation from the ancillary ligands, in particular when the added groups are fully or partially oriented trans to X. The resulting trans interaction is a very strong effect, much stronger than the weak antibonding  $\pi$ -interactions. Thus, the reaction is strongly disfavored by increasing  $\sigma$ -donation from X. The concept of “oxidative” addition (or reductive addition<sup>13</sup>) is therefore misleading, as it focuses on the overall change of charge, rather than the more specific and important question of how the charge distribution on the metal center is affected by the reaction.

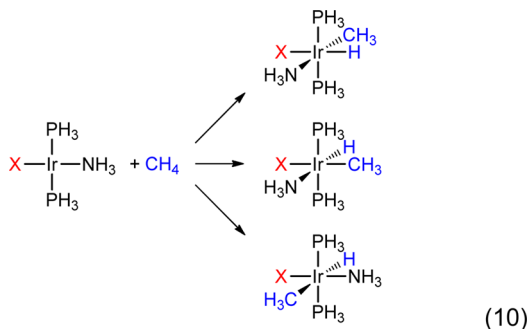
The formation of 3c-2e bonds as a result of OA is consistent with the view that transition metal complexes with more than 12 valence electrons may be characterized as hypervalent.<sup>91</sup> We also note that although decreased electron donation by ancillary ligands tends to favor the additions (opposite the expectation based upon a reaction being “oxidative”) this description implies, in accord with the results of numerous studies,<sup>52,81,93–97</sup> that oxidative addition should also be favored by electron-withdrawing substrates on the addendum (consistent with the reaction being “oxidative”). Electron-withdrawing substrates of course will significantly favor the energetics of eq 5 (electron transfer) while their effect on eq 6 should be mixed; greater basicity of  $A^-$  or  $B^-$  favors the coordination of these anions, but that coordination comes at a price of decreasing the strength of the metal–ligand (e.g., M–X) bonds that are present prior to coordination of  $A^-$  or  $B^-$ .

As noted above, C–H addition to Ir( $PH_3$ )<sub>2</sub>X is more favorable by ca. 30 kcal/mol for X = F vs X = H. If the reaction is viewed in terms of oxidation or reduction, this trend would suggest that the energetics are dominated by a reductive component (at least in the electron-poor system, i.e., X = F). In that case electron-poor substrates would add less favorably. In fact, C–H bonds of electron-poor alkyl groups are calculated to undergo addition to Ir( $PH_3$ )<sub>2</sub>F even more favorably than those of unsubstituted alkanes. For example, the energy of addition of the C–H bond at the  $\beta$ -carbon of fluoroethane or trifluoroethane is more favorable than that for addition of ethane (eqs 7 and 8). Addition of the C–H bond  $\alpha$  to fluorine in

fluoromethane also is more favorable than addition of methane, and by an even greater amount (eq 9), although the thermodynamics in this case are perhaps less meaningful because they could be attributed to the greater  $\pi$ -accepting ability of the  $\alpha$ -F-substituted C atom, or rehybridization engendered by the  $\alpha$ -substitution.<sup>98</sup> Thus, the OA reactions are favored both by more electron-poor ancillary ligands and by more electron-poor addenda, indicating that overall charge transfer (in either direction) does not strongly contribute to the reaction thermodynamics.



**Oxidative Addition of Methane to Four-Coordinate Ir(I) Complexes.** The approach used above to analyze C–H addition to three-coordinate Ir(I) has also been applied to C–H addition to four-coordinate Ir(I) complexes, the archetypal class of complexes that undergo oxidative addition. In this case, all the ancillary ligands are positioned fully trans to another ligand in both the reactant and product. Thus, to a first approximation the trans influence is not expected to play an important role in the analysis. We find, however, that the principles elucidated above, and even the particular importance of the trans influence, are applicable, and our results can be rationalized in similar terms for both three- and four-coordinate complexes. As a “generic” fourth ligand we chose  $\text{NH}_3$ , and we investigated the effect of varying the electronic properties of X on the energy of methane C–H addition to *trans*-( $\text{PH}_3$ )<sub>2</sub>IrX-( $\text{NH}_3$ ) (eq 10).



Linear regression analysis was applied to the formation energies of each isomer of the six-coordinate reaction product, providing three regression equations (Table 8). The regression analyses for the two reactions that yield a *cis*-C–H addition product (the typical mode for oxidative addition of covalent bonds) afford positive values of  $C_\sigma$  and negative values of  $C_\pi$ , as was generally found for oxidative addition to three-coordinate Ir(I). Analogously to the 3- $\text{T}_\text{H}$  SQP geometry, the ligands of the six-coordinate oxidative addition products may be

considered to interact with  $sd^2$ -hybridized metal orbitals that are oriented along the three metal–ligand bond axes. In the case of addition to form the products in which the hydride and methyl groups are *cis* to each other, more strongly  $\sigma$ -donating X ligands disfavor oxidative addition due to the replacement of a neutral ligand ( $\text{NH}_3$ ) in the position *trans* to X in the reactant, with a strong *trans*-influence ligand (hydride or methyl) in the six-coordinate product. The values of  $C_\sigma$  and  $C_\pi$  are similar for formation of the two isomeric *cis*-C–H addition products, not surprisingly since methyl and H have comparable *trans* influences.

The signs of  $C_\sigma$  and  $C_\pi$  are reversed when oxidative addition proceeds in a *trans*-fashion ( $C_\sigma = -32$  and  $C_\pi = +42$ ; Table 8). This reversal is consistent with the orbital rationale presented above for oxidative addition to three-coordinate Ir(I) to give five-coordinate SQP 3- $\text{T}_\text{X}$ . In the six-coordinate case, the  $\text{NH}_3$  group is positioned *trans* to the X ligand in both reactant and product, as is the vacant coordination site in the case of addition to give 3- $\text{T}_\text{X}$ . Accordingly, the multivariable linear regression for *trans* addition to *trans*-( $\text{PH}_3$ )<sub>2</sub>IrX( $\text{NH}_3$ ) closely resembles that for addition to give 3- $\text{T}_\text{X}$ .  $C_\sigma$  is again small and negative (cf.  $-38$  for formation of 3- $\text{T}_\text{X}$ ); again, this result may relate to an antibonding interaction of X with the torus of the filled  $5d_z^2$  orbital in the reactant.

**Oxidative Addition of the N–H Bond of Ammonia to Three-Coordinate Ir(I) Complexes.** There are few examples of oxidative addition of ammonia that yield an amido hydride complex,<sup>34–42</sup> only two of which constitute oxidative addition of ammonia to a single, well-defined late transition metal center.<sup>36,38</sup> In 2005, we reported that the aliphatic PCP pincer iridium propene complex **8** reacts with ammonia to give amido hydride **9** at 25 °C (Scheme 5),<sup>36</sup> whereas the independently synthesized iridium amido hydride complex **10**, containing the less electron-donating aryl PCP pincer ligand, underwent isomerization to the four-coordinate ammine complex **11** at 25 °C. These observations, and Turculet’s report that oxidative addition of ammonia occurs to an iridium pincer complex bearing a strongly  $\sigma$ -donating PSiP ligand,<sup>38</sup> seemed in accord with the commonly held view that oxidative addition is favored by a more electron-rich metal center. We therefore investigated the electronic effects on the oxidative addition of ammonia by the same approach as we used to study the electronic effects on the oxidative addition of methane.

The reaction energies for oxidative addition of  $\text{NH}_3$  to a variety of three-coordinate ( $\text{PH}_3$ )<sub>2</sub>IrX complexes were calculated (Table 9),<sup>99</sup> and a multivariable linear regression was performed (Table 10).  $C_\sigma$  was found to be positive ( $69 \pm 9$ ), indicating that N–H addition, like C–H addition, is *disfavored* by more strongly  $\sigma$ -donating ligands, in apparent contradiction to the observations noted above.

However, the same type of analysis, when applied to simple  $\text{NH}_3$  coordination to *trans*-( $\text{PH}_3$ )<sub>2</sub>IrX,<sup>100,101</sup> reveals that increased  $\sigma$ -donation by X disfavors N-coordination even more strongly than it disfavors N–H addition (Tables 9 and 10). The coefficients for both reactions are substantial and positive (i.e., both reactions are disfavored by increased  $\sigma$ -donation by X), but the coefficient for  $\text{NH}_3$  coordination ( $105 \pm 9$ ) significantly exceeds that for N–H oxidative addition ( $69 \pm 9$ ). Thus, while increased  $\sigma$ -donation by the ancillary ligand X clearly *disfavors* OA in an absolute sense, it favors N–H addition relative to simple nitrogen coordination.

The  $\pi_\text{X}$  coefficient in the regression equation for  $\text{NH}_3$  coordination ( $C_\pi = 41 \pm 16$ ) is essentially equal to the  $\pi_\text{X}$

Table 8. Regression Equations for Methane Addition to  $(\text{PH}_3)_2\text{IrX}(\text{NH}_3)$  Based on Constrained Geometries

reaction / product isomer	regression equation	SD <sup>a</sup> of $\sigma$ effects (kcal/mol)	SD <sup>a</sup> of $\pi$ effects (kcal/mol)
	$\Delta E_X = (44 \pm 7)\sigma_X + (-23 \pm 13)\pi_X + (-1 \pm 1)$	+4.5	-1.2
	$\Delta E_X = (49 \pm 10)\sigma_X + (-36 \pm 18)\pi_X + (1 \pm 1)$	+5.3	-2.1
	$\Delta E_X = (-32 \pm 6)\sigma_X + (42 \pm 11)\pi_X + (2 \pm 1)$	-3.4	+2.5

<sup>a</sup>SD = standard deviation. The sign (+ or -) of a particular regression coefficient determines the direction of the effect: a positive value indicates that increased electron donation disfavors the reaction and hence increases the energy of addition.

### Scheme 5. Formation and Subsequent Reactivity of (PCP)Ir Amido Hydride Complexes.

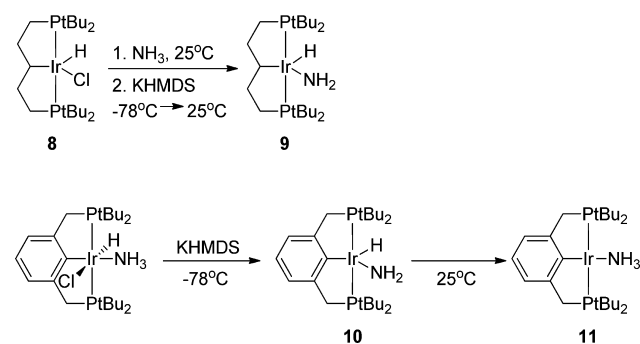


Table 9.  $\sigma_X$  Values and Calculated Reaction Energies ( $\Delta E_X$ , kcal/mol) for  $\text{NH}_3$  Oxidative Addition and Coordination to  $\text{trans}-(\text{PH}_3)_2\text{IrX}^a$

X ligand	$\sigma_X$	$\Delta E_{\text{NH}_3}$ oxidative addition	$\Delta E_{\text{NH}_3}$ coordination
$\text{BH}_3^{2-}$	0.235	-9.1	-0.2
$\text{BH}_2^-$ ,	0.139	-15.6	-12.5
$\text{Li}^-$	0.128	-12.9	-4.3
$\text{BH}_2^-$ , $\perp$	0.115	-7.3	-12.8
$\text{O}^{2-}$	0.023	-7.5	-11.9
$\text{H}^-$	0.000	-22.9	-21.6
$\text{Ph}^-$ , $\perp$	-0.012	-18.0	-21.3
$\text{CH}_3^-$	-0.015	-20.1	-21.8
$\text{CF}_3^-$	-0.033	-21.5	-25.2
$\text{NO}_2^-$ ,	-0.071	-22.1	-28.0
$\text{NH}_2^-$ , $\perp^b$	-0.072	-24.2	-26.4
$\text{NH}_2^-$ ,    <sup>c</sup>	-0.072	-19.2	-28.1
$\text{NO}_2^-$ , $\perp$	-0.081	-21.2	-26.5
$\text{OMe}^-$ , $\perp$	-0.106	-27.3	-30.0
pyrrolide, $\perp$	-0.108	-29.6	-33.4
$\text{OH}^-$ , $\perp$	-0.110	-27.9	-32.4
$\text{OH}^-$ ,	-0.113	-27.8	-32.8
$\text{OMe}^-$ ,	-0.113	-26.9	-32.3
$\text{F}^-$	-0.146	-35.4	-39.3
$\text{NH}_3$	-0.153	-40.9	-53.1

<sup>a</sup>|| = parallel to P-Ir-P axis.  $\perp$  = perpendicular to P-Ir-P axis. <sup>b</sup>H-N-Ir-P dihedral angles set to 58.5°. <sup>c</sup>H-N-Ir-P dihedral angles set to 31.5°.

coefficient for  $\text{NH}_3$  oxidative addition ( $43 \pm 17$ ), indicating that  $\pi$  effects do not significantly favor or disfavor  $\text{NH}_3$  coordination vs oxidative N-H addition.

### SUMMARY

Results from DFT calculations indicate that C-H or N-H oxidative addition to three-coordinate  $\text{trans}-(\text{PH}_3)_2\text{IrX}$  complexes is generally favored by the presence of a *less*  $\sigma$ -donating ligand (X) trans to the coordination site of addition; the magnitude of this thermodynamic effect can be large. While these results contradict a deeply rooted view that OA should be favored by strongly electron-donating ligands, they can be explained in a fairly straightforward manner. Oxidative addition to 14e  $\text{trans}-(\text{PH}_3)_2\text{IrX}$  (a typical late metal fragment) may be viewed in terms of (i) transfer of electron density from nonbonding metal d-orbitals, followed by (ii) addition of the reduced addendum fragments which donate electron density into orbitals already accepting electron density from the ancillary ligands, i.e.  $\sigma$ -antibonding orbitals. Addition of these formally reduced fragments to form 3c-2e bonds is particularly disfavored by greater  $\sigma$ -donation from the ligand trans to the site of the addition.

Experimentally, our explanation is supported by the large differences observed in the enthalpy or free energy of activation for reductive elimination from five-coordinate Ir(III) phenyl hydride complexes to form the C-H bond of benzene. The barrier to elimination of benzene from a site trans to a chloride is much greater than that for elimination from a site trans to a PCP-pincer aryl or a PSiP-pincer silyl group; the barrier to elimination from a site trans to a N-coordinating group, which can be either strongly (amido) or weakly (pyridyl)  $\pi$ -donating, is between these two extremes.

The same computational methods have been used to investigate oxidative addition to  $\text{cis}-(\text{PH}_3)_2\text{IrX}$ . In this case neither the orbitals that are vacated nor the orbitals that accept electron density from the reduced fragments (according to the model noted above) are strongly involved in bonding with the ligand X. Accordingly, the thermodynamics of OA are found to be much less sensitive to the nature of X, particularly its strength as a  $\sigma$ -donor, when the ligand X is cis to the site of addition.

Oxidative addition of methane to a four-coordinate Ir(I) complex,  $\text{trans}-(\text{PH}_3)_2\text{Ir}(\text{NH}_3)\text{X}$ , to afford either of two possible cis methyl-hydride (*trans*-phosphine) adducts is found to be weakly disfavored by increased  $\sigma$ -donation by



Table 10. Regression Equations for the Oxidative Addition and Coordination of NH<sub>3</sub> to *trans*-(PH<sub>3</sub>)<sub>2</sub>IrX Using Constrained Geometries

reaction / product isomer	regression equation	SD <sup>a</sup> of $\sigma$ effects (kcal/mol)	SD <sup>a</sup> of $\pi$ effects (kcal/mol)
 $\text{X}-\text{Ir}(\text{PH}_3)_2 + \text{NH}_3 \rightarrow \text{H}_2\text{N}-\text{Ir}(\text{PH}_3)_2\text{X}$ N-H oxidative addition	$\Delta E_x = (69 \pm 9)\sigma_x + (43 \pm 17)\pi_x + (-21 \pm 1)$	+7.3	+2.5
 $\text{X}-\text{Ir}(\text{PH}_3)_2 + \text{NH}_3 \rightarrow \text{X}-\text{Ir}(\text{PH}_3)_2\text{NH}_3$ NH <sub>3</sub> coordination	$\Delta E_x = (105 \pm 9)\sigma_x + (41 \pm 16)\pi_x + (-23 \pm 1)$	+11.3	+2.4

<sup>a</sup>SD = standard deviation. The sign (+ or -) of a particular regression coefficient indicates the direction of the effect; a positive value indicates that increased electron donation disfavors the reaction and increases the energy of addition.

ligands X. This trend is attributable to the replacement of NH<sub>3</sub> in the six-coordinate product by a stronger *trans*-influence ligand, either methyl or hydride, in the position *trans* to X. By contrast, addition of the C–H bond in a *trans* fashion is favored, but only weakly, by increased  $\sigma$ -donation by X.

Thus, the widely accepted view that OA is favored by more strongly electron-donating ligands does not appear to be generally valid for addition of C–H bonds. Similar conclusions are reached for the addition of the N–H bond of ammonia. These conclusions are, presumably, general for species that form bonds with the metal that are largely covalent. Addition of such species should not be regarded primarily in terms of oxidation (or reduction) but is best viewed in terms of a redistribution of electron density;<sup>102</sup> accordingly, the energetics are influenced by the individual electronic components ( $\sigma$  and  $\pi$ ) of the ancillary ligands in ways that vary with each set of reactants and products. In general, we predict that when OA results in a change in occupancy at the site *trans* to any ancillary ligand X, the dominant effect of varying the ancillary ligand will result from varying its *trans* influence. For oxidative additions of A–B that form products in which the ligand A or B lies *trans* to an ancillary ligand, and in which ligands A and B are bound to the metal through largely covalent bonds, the thermodynamics of OA will be more favorable for those complexes in which the ancillary ligand is a weaker  $\sigma$  donor.

## ■ ASSOCIATED CONTENT

### Supporting Information

The Supporting Information is available free of charge on the ACS Publications website at DOI: 10.1021/jacs.5b09522.

Computational data (PDF)

Experimental procedures, characterization data (PDF)

## ■ AUTHOR INFORMATION

### Corresponding Authors

\*kroghjes@rutgers.edu (K.K.-J.)

\*alan.goldman@rutgers.edu (A.S.G.)

### Notes

The authors declare no competing financial interest.

## ■ ACKNOWLEDGMENTS

This work was supported by the National Science Foundation through Grant CHE-1465203 and through the CCI Center for Enabling New Technologies through Catalysis (CENTC), Grant CHE-1205189. Odile Eisenstein is thanked for very helpful discussions and suggestions. Oleg Ozerov and co-

workers are thanked for generously providing PNP ligand, as well as stimulating discussions on the subject of this work.

## ■ REFERENCES

- (1) Collman, J. P. *Acc. Chem. Res.* **1968**, *1*, 136–143.
- (2) Labinger, J. A. *Organometallics* **2015**, *34*, 4784–4795.
- (3) Chen, Q.-A.; Ye, Z.-S.; Duan, Y.; Zhou, Y.-G. *Chem. Soc. Rev.* **2013**, *42*, 497–511.
- (4) Morris, R. H. *Chem. Soc. Rev.* **2009**, *38*, 2282–2291.
- (5) Wu, X.-F.; Neumann, H.; Beller, M. *Chem. Rev.* **2013**, *113*, 1–35.
- (6) Barnard, C. F. J. *Organometallics* **2008**, *27*, 5402–5422.
- (7) Ackermann, L., Ed. *Modern Arylation Methods*; Wiley-VCH Verlag GmbH & Co. KGaA: Weinheim, 2009.
- (8) Seechurn, C. C. C. J.; Kitching, M. O.; Colacot, T. J.; Snieckus, V. *Angew. Chem., Int. Ed.* **2012**, *51*, 5062–5085.
- (9) Magano, J.; Dunetz, J. R. *Chem. Rev.* **2011**, *111*, 2177–2250.
- (10) Saillard, J.; Hoffmann, R. *J. Am. Chem. Soc.* **1984**, *106*, 2006–2026.
- (11) Low, J. J.; Goddard, W. A., III *J. Am. Chem. Soc.* **1986**, *108*, 6115–6128.
- (12) Koga, N.; Morokuma, K. *J. Phys. Chem.* **1990**, *94*, 5454–5462.
- (13) Crabtree, R. H.; Quirk, J. M. *J. Organomet. Chem.* **1980**, *199*, 99–106.
- (14) Collman, J. P.; Hegedus, L. S.; Norton, J. R.; Finke, R. G. *Principles and Applications of Organotransition Metal Chemistry*; University Science Books: Mill Valley, CA, 1987; pp 279–305.
- (15) Cotton, F. A.; Wilkinson, G.; Murillo, C. A.; Bochmann, M.; *Advanced Inorganic Chemistry*, 6th ed.; John Wiley & Sons: New York, 1999, p 1171–1177.
- (16) Hartwig, J. F. *Organotransition Metal Chemistry*; University Science Books: Sausalito, CA, 2010; pp 261–300.
- (17) Crabtree, R. H. *The Organometallic Chemistry of the Transition Metals*, 6th ed.; John Wiley & Sons, Inc.: Hoboken, NJ, 2014; pp 163–168.
- (18) Su, M.-D.; Chu, S.-Y. *J. Phys. Chem. A* **1998**, *102*, 10159–10166.
- (19) Su, M.-D.; Chu, S.-Y. *Inorg. Chem.* **1998**, *37*, 3400–3406.
- (20) Fazaeli, R.; Ariafard, A.; Jamshidi, S.; Tabatabaie, E. S.; Pishro, K. A. *J. Organomet. Chem.* **2007**, *692*, 3984–3993.
- (21) Hartwig, J. F. *Inorg. Chem.* **2007**, *46*, 1936–1947.
- (22) Ariafard, A.; Yates, B. F. *J. Organomet. Chem.* **2009**, *694*, 2075–2084.
- (23) Yamashita, M.; Vicario, J. V. C.; Hartwig, J. F. *J. Am. Chem. Soc.* **2003**, *125*, 16347–16360.
- (24) Some reviews of alkane C–H bond activation by organometallic complexes: (a) Jones, W. D. *Science* **2000**, *287*, 1942–1943. (b) Labinger, J. A.; Bercaw, J. E. *Nature* **2002**, *417*, 507–514. (c) Crabtree, R. H. *J. Organomet. Chem.* **2004**, *689*, 4083–4091. (d) Goldberg, K. I.; Goldman, A. S., Eds. *Activation and Functionalization of C–H Bonds*; ACS Symposium Series 885; American Chemical Society: Washington, DC, 2004. [http://rutchem.rutgers.edu/~agoldman/TOC\\_ACS\\_Symposium\\_Series\\_885.htm](http://rutchem.rutgers.edu/~agoldman/TOC_ACS_Symposium_Series_885.htm) (e) Bergman, R. G. *Nature* **2007**, *446*, 506. (f) Crabtree, R. H. *Chem.*

- Rev. **2010**, *110*, 575. (g) Balcells, D.; Clot, E.; Eisenstein, O. *Chem. Rev.* **2010**, *110*, 749–823. (h) Lyons, T. W.; Sanford, M. S. *Chem. Rev.* **2010**, *110*, 1147–1169.
- (25) Kubas, G. J. *Chem. Rev.* **2007**, *107*, 4152–4205.
- (26) Dub, P. A.; Belkova, N. V.; Filippov, O. A.; Daran, J.-C.; Epstein, L. M.; Lledós, A.; Shubina, E. S.; Poli, R. *Chem. - Eur. J.* **2010**, *16*, 189–201.
- (27) Baya, M.; Esteruelas, M. A.; Oliván, M.; Oñate, E. *Inorg. Chem.* **2009**, *48*, 2677–2686.
- (28) Hebden, T. J.; St. John, A. J.; Gusev, D. G.; Kaminsky, W.; Goldberg, K. I.; Heinekey, D. M. *Angew. Chem., Int. Ed.* **2011**, *50*, 1873–1876.
- (29) Chaplin, A. B.; Weller, A. S. *Organometallics* **2011**, *30*, 4466–4469.
- (30) Tsay, C.; Peters, J. C. *Chem. Sci.* **2012**, *3*, 1313–1318.
- (31) Connelly, S. J.; Zimmerman, A. C.; Kaminsky, W.; Heinekey, D. M. *Chem. - Eur. J.* **2012**, *18*, 15932–15934.
- (32) Grellier, M.; Mason, S. A.; Albinati, A.; Capelli, S. C.; Rizzato, S.; Bijani, C.; Coppel, Y.; Sabo-Etienne, S. *Inorg. Chem.* **2013**, *52*, 7329.
- (33) Hebden, T. J.; Goldberg, K. I.; Heinekey, D. M.; Zhang, X.; Emge, T. J.; Goldman, A. S.; Krogh-Jespersen, K. *Inorg. Chem.* **2010**, *49*, 1733–1742.
- (34) Hillhouse, G. L.; Bercaw, J. E. *J. Am. Chem. Soc.* **1984**, *106*, 5472–5478.
- (35) Casalnuovo, A. L.; Calabrese, J. C.; Milstein, D. *Inorg. Chem.* **1987**, *26*, 971–3.
- (36) Zhao, J.; Goldman, A. S.; Hartwig, J. F. *Science* **2005**, *307*, 1080–1082.
- (37) Nakajima, Y.; Kameo, H.; Suzuki, H. *Angew. Chem., Int. Ed.* **2006**, *45*, 950–952.
- (38) Morgan, E.; MacLean, D. F.; McDonald, R.; Turculet, L. *J. Am. Chem. Soc.* **2009**, *131*, 14234–14236.
- (39) Salomon, M. A.; Jungton, A.-K.; Braun, T. *Dalton Trans.* **2009**, 7669–7677.
- (40) Khaskin, E.; Iron, M. A.; Shimon, L. J. W.; Zhang, J.; Milstein, D. *J. Am. Chem. Soc.* **2010**, *132*, 8542–8543.
- (41) Velez, E.; Betore, M. P.; Casado, M. A.; Polo, V. *Organometallics* **2015**, *34*, 3959–3966.
- (42) McCarthy, S. M.; Lin, Y.-C.; Devarajan, D.; Chang, J. W.; Yennawar, H. P.; Rioux, R. M.; Ess, D. H.; Radosevich, A. T. *J. Am. Chem. Soc.* **2014**, *136*, 4640–4650.
- (43) Vaska, L.; DiLuzio, J. W. *J. Am. Chem. Soc.* **1962**, *84*, 679–80.
- (44) Vaska, L. *Acc. Chem. Res.* **1968**, *1*, 335–44.
- (45) We are not aware of examples of intermolecular addition of unactivated  $sp^2$  or  $sp^3$  C–H bonds to well characterized square planar complexes to give simple addition products. Addition to highly electron-rich four-coordinate  $d^8$  complexes has played a seminal role in the development of C–H activation (a, b), but such complexes have been reported to have geometric and electronic structures very different from those of square planar complexes (c–e): (a) Chatt, J.; Davidson, J. M. *J. Chem. Soc.* **1965**, 843–855. (b) Ittel, S. D.; Tolman, C. A.; English, A. D.; Jesson, J. P. *J. Am. Chem. Soc.* **1976**, *98*, 6073–6075. (c) Whittlesey, M. K.; Mawby, R. J.; Osman, R.; Perutz, R. N.; Field, L. D.; Wilkinson, M. P.; George, M. W. *J. Am. Chem. Soc.* **1993**, *115*, 8627. (d) Cronin, L.; Nicasio, M. C.; Perutz, R. N.; Peters, R. G.; Roddick, D. M.; Whittlesey, M. K. *J. Am. Chem. Soc.* **1995**, *117*, 10047. (e) Macgregor, S. A.; Eisenstein, O.; Whittlesey, M. K.; Perutz, R. N. *J. Chem. Soc., Dalton Trans.* **1998**, 291.
- (46) For examples of addition of acidic C–H bonds to four-coordinate  $d^8$  complexes (a–c), also reported (d) to deviate substantially from a square planar geometry, see: (a) English, A. D.; Herskovitz, T. *J. Am. Chem. Soc.* **1977**, *99*, 1648–1649. (b) Marder, T. B.; Zargarian, D.; Calabrese, J. C.; Herskovitz, T. H.; Milstein, D. *J. Chem. Soc., Chem. Commun.* **1987**, 1484–1485. (c) Crestani, M. G.; Steffen, A.; Kenwright, A. M.; Batsanov, A. S.; Howard, J. A. K.; Marder, T. B. *Organometallics* **2009**, *28*, 2904–2914. (d) Blum, O.; Calabrese, J. C.; Frolow, F.; Milstein, D. *Inorg. Chim. Acta* **1990**, *174*, 149–151.
- (47) For an example of  $sp^2$  C–H addition to a square planar complex yielding an unobserved intermediate, see: Nuckel, S.; Burger, P. *Angew. Chem., Int. Ed.* **2003**, *42*, 1632–1636.
- (48) For addition of an alkynyl C–H bond to a square planar  $d^8$  complex, (PCP)Ir(CO), see: Hackenberg, J. D.; Kundu, S.; Emge, T. J.; Krogh-Jespersen, K.; Goldman, A. S. *J. Am. Chem. Soc.* **2014**, *136*, 8891–8894.
- (49) Goldman, A. S.; Goldberg, K. I. In *Activation and Functionalization of C–H Bonds*; Goldberg, K. I., Goldman, A. S., Eds.; ACS Symposium Series 885; American Chemical Society: Washington, DC, 2004; pp 1–43.10.1021/bk-2004-0885.ch001
- (50) Cundari, T. R. *J. Am. Chem. Soc.* **1994**, *116*, 340–347 and references therein.
- (51) Xu, W.; Rosini, G. P.; Gupta, M.; Jensen, C. M.; Kaska, W. C.; Krogh-Jespersen, K.; Goldman, A. S. *Chem. Commun.* **1997**, 2273–2274.
- (52) Krogh-Jespersen, K.; Czerw, M.; Zhu, K.; Singh, B.; Kanzelberger, M.; Darji, N.; Achord, P. D.; Renkema, K. B.; Goldman, A. S. *J. Am. Chem. Soc.* **2002**, *124*, 10797–10809.
- (53) Krogh-Jespersen, K.; Goldman, A. S. In *Transition State Modeling for Catalysis*; Truhlar, D. G., Morokuma, K., Eds.; American Chemical Society: Washington, DC, 1999; pp 151–162.
- (54) Su, M.-D.; Chu, S.-Y. *J. Am. Chem. Soc.* **1997**, *119*, 10178–10185.
- (55) Macgregor, S. A. *Organometallics* **2001**, *20*, 1860–1874.
- (56) Diggle, R. A.; Macgregor, S. A.; Whittlesey, M. K. *Organometallics* **2004**, *23*, 1857–1865.
- (57) Parr, R. G.; Yang, W. *Density-Functional Theory of Atoms and Molecules*; University Press: Oxford, 1989.
- (58) (a) Frisch, M. J. et al. *Gaussian 03*; Gaussian, Inc.: Wallingford, CT, 2004. (b) Frisch, M. J. et al. *Gaussian 09*; Gaussian, Inc.: Wallingford, CT, 2009. See the [Supporting Information](#) for the complete references to Gaussian 03 and Gaussian 09.
- (59) Perdew, J. P.; Burke, K.; Ernzerhof, M. *Phys. Rev. Lett.* **1996**, *77*, 3865–3868.
- (60) Dolg, M.; Wedig, U.; Stoll, H.; Preuss, H. *J. Chem. Phys.* **1987**, *86*, 866–72.
- (61) Ditchfield, R.; Hehre, W. J.; Pople, J. A. *J. Chem. Phys.* **1971**, *54*, 724–728.
- (62) Hariharan, P. C.; Pople, J. A. *Mol. Phys.* **1974**, *27*, 209–214.
- (63) Krishnan, R.; Binkley, J. S.; Seeger, R.; Pople, J. A. *J. Chem. Phys.* **1980**, *72*, 650–654.
- (64) Clark, T.; Chandrasekhar, J.; Spitznagel, G. W.; Schleyer, P. v. R. *J. Comput. Chem.* **1983**, *4*, 294–301.
- (65) Hay, P. J.; Wadt, W. R. *J. Chem. Phys.* **1985**, *82*, 299–310.
- (66) Roy, L. E.; Hay, P. J.; Martin, R. L. *J. Chem. Theory Comput.* **2008**, *4*, 1029–1031.
- (67) Reed, A. E.; Curtiss, L. A.; Weinhold, F. *Chem. Rev.* **1988**, *88*, 899–926.
- (68) Carpenter, J. E.; Weinhold, F. *J. Mol. Struct.: THEOCHEM* **1988**, *169*, 41–62.
- (69) Glendening, E. D.; Badenhop, J. K.; Reed, A. E.; Carpenter, J. E.; Bohmann, J. A.; Morales, C. M.; Weinhold, F. *NBO 5.0*; Theoretical Chemistry Institute, University of Wisconsin: Madison, WI, 2001 (<http://www.chem.wisc.edu/~nbo5>).
- (70) Huheey, J. E. *Inorganic Chemistry*, 3rd ed.; Harper and Row: New York, 1983.
- (71) The exception to this was  $NH_2^-$ , since the  $IrNH_2$  unit is nonplanar. The H–N–Ir–P dihedral angles were set to  $58.5^\circ$  and  $31.5^\circ$  for “perpendicular” and “parallel” orientations, respectively.
- (72) Large differences in geometrical parameters between unconstrained and partially constrained complexes typically arise from the introduction of a ‘chemically unconventional’ substituent such as X = Li, where the unconstrained 1-Li geometry has an optimized P–Ir–P angle of  $127^\circ$ . The average difference in Ir–X bond length becomes 0.035 Å.
- (73) For insightful discussions of the relative importance of  $\pi$ -backbonding by various ligands, see, for example: (a) Harvey, J. N.; Heslop, K. M.; Orpen, A. G.; Pringle, P. G. *Chem. Commun.* **2003**, 278–279.

- (b) Leyssens, T.; Peeters, D.; Orpen, A. G.; Harvey, J. N. *New J. Chem.* **2005**, *29*, 1424–1430. (c) Leyssens, T.; Peeters, D.; Orpen, A. G.; Harvey, J. N. *Organometallics* **2007**, *26*, 2637–2645.
- (74) The calculated energies ( $E$ ) refer to electronic energy (the internal energy without vibrational or thermal corrections). Meaningful values of enthalpy ( $H$ ) and Gibbs free energy ( $G$ ) can only be calculated at stationary points on the potential energy surface, whereas most of the complexes used for parametrization purposes in this work contain structural constraints. Moreover, since we are interested in electronic substituent effects, determination of the correlation with electronic energy is perhaps intrinsically more appropriate than correlation with values of  $\Delta H$  or  $\Delta G$ . We have calculated the values of  $\Delta H$  and  $\Delta G$  only for reactions that involve direct comparison with experimental values, such as elimination of benzene from (pincer)Ir phenyl hydride complexes.
- (75) Jean, Y.; Eisenstein, O. *Polyhedron* **1988**, *7*, 405–407.
- (76) Rachidi, I. E. I.; Eisenstein, O.; Jean, Y. *New J. Chem.* **1990**, *14*, 671–677.
- (77) Riehl, J. F.; Jean, Y.; Eisenstein, O.; Pelissier, M. *Organometallics* **1992**, *11*, 729–737.
- (78) Sola, E.; Garcia-Camprubi, A.; Andres, J. L.; Martin, M.; Plou, P. *J. Am. Chem. Soc.* **2010**, *132*, 9111–9121.
- (79) Kanzelberger, M.; Singh, B.; Czerw, M.; Krogh-Jespersen, K.; Goldman, A. S. *J. Am. Chem. Soc.* **2000**, *122*, 11017–11018.
- (80) (a) Fan, L.; Foxman, B. M.; Ozerov, O. V. *Organometallics* **2004**, *23*, 326–328. (b) Fan, L.; Yang, L.; Guo, C.; Foxman, B. M.; Ozerov, O. V. *Organometallics* **2004**, *23*, 4778–4787. (c) Ozerov, O. V.; Guo, C.; Fan, L.; Foxman, B. M. *Organometallics* **2004**, *23*, 5573–5580. (d) Ozerov, O. V.; Guo, C.; Papkov, V. A.; Foxman, B. M. *J. Am. Chem. Soc.* **2004**, *126*, 4792–4793. (e) Fan, L.; Parkin, S.; Ozerov, O. V. *J. Am. Chem. Soc.* **2005**, *127*, 16772–16773.
- (81) Ben-Ari, E.; Gandelman, M.; Rozenberg, H.; Shimon, L. J. W.; Milstein, D. *J. Am. Chem. Soc.* **2003**, *125*, 4714–4715.
- (82) Ben-Ari, E.; Cohen, R.; Gandelman, M.; Shimon, L. J. W.; Martin, J. M. L.; Milstein, D. *Organometallics* **2006**, *25*, 3190–3210.
- (83) Werner, H.; Höhn, A.; Dziallas, M. *Angew. Chem., Int. Ed. Engl.* **1986**, *25*, 1090–1092.
- (84) Rosini, G. P.; Wang, K.; Patel, B.; Goldman, A. S. *Inorg. Chim. Acta* **1998**, *270*, 537–542.
- (85) Attempts at locating a conventional TS for reductive coupling of benzene from **5-HPh** employing DFT failed uniformly. Several functional/basis set combinations were applied to the problem to no avail; we could, however, locate a proper  $\text{TS}_{\text{RC-HPh}}$  using Hartree–Fock (HF) theory. A best estimate for the potential energy barrier associated with benzene reductive coupling in **5-HPh** was thus obtained from single point PBE calculations on the HF optimized structures for **5-HPh** and  $\text{TS}_{\text{RC-HPh}}$ ; thermal corrections computed at the HF level for **5-HPh** and  $\text{TS}_{\text{RC-HPh}}$  were then applied to obtain the  $\Delta H_{\text{RC-DFT}}^\ddagger$  and  $\Delta G_{\text{RC-DFT}}^\ddagger$  values shown in Table 6.
- (86) MacLean, D. F.; McDonald, R.; Ferguson, M. J.; Caddell, A. J.; Turculet, L. *Chem. Commun.* **2008**, 5146–5148.
- (87) Chatt, J.; Shaw, B. L. *J. Chem. Soc.* **1959**, 4020–33.
- (88) Sakaki, S.; Kai, S.; Sugimoto, M. *Organometallics* **1999**, *18*, 4825–4837.
- (89) Takagi, N.; Sakaki, S. *J. Am. Chem. Soc.* **2012**, *134*, 11749–11759.
- (90) (a) Landis, C. R.; Firman, T. K.; Root, D. M.; Cleveland, T. J. *J. Am. Chem. Soc.* **1998**, *120*, 1842–1854. (b) Landis, C. R.; Cleveland, T.; Firman, T. K. *J. Am. Chem. Soc.* **1998**, *120*, 2641–2649.
- (91) Weinhold, F.; Landis, C. R. *Valency and bonding: a natural bond orbital donor-acceptor perspective*; Cambridge University Press: Cambridge, 2005.
- (92) Frenking, G.; Froehlich, N. *Chem. Rev.* **2000**, *100*, 717–774.
- (93) (a) Evans, M. E.; Burke, C. L.; Yaibuathes, S.; Clot, E.; Eisenstein, O.; Jones, W. D. *J. Am. Chem. Soc.* **2009**, *131*, 13464–13473. (b) Evans, M. E.; Li, T.; Vetter, A. J.; Rieth, R. D.; Jones, W. D. *J. Org. Chem.* **2009**, *74*, 6907–6914. (c) Tanabe, T.; Brennessel, W. W.; Clot, E.; Eisenstein, O.; Jones, W. D. *Dalton Trans.* **2010**, *39*, 10495–10509. (d) Jiao, Y.; Evans, M. E.; Morris, J.; Brennessel, W. W.; Jones, W. D. *J. Am. Chem. Soc.* **2013**, *135*, 6994–7004.
- (94) Puri, M.; Gatard, S.; Smith, D. A.; Ozerov, O. V. *Organometallics* **2011**, *30*, 2472–2482.
- (95) Sakaki, S.; Biswas, B.; Sugimoto, M. *Organometallics* **1998**, *17*, 1278–1289.
- (96) Shekhar, S.; Hartwig, J. F. *J. Am. Chem. Soc.* **2004**, *126*, 13016–13027.
- (97) Lam, K. C.; Marder, T. B.; Lin, Z. *Organometallics* **2007**, *26*, 758–760.
- (98) Albeniz, A. C.; Casares, J. A. *Advances in Organometallic Chemistry*, Vol. 62; Elsevier Academic Press Inc: San Diego, 2014; Vol. 62, pp 1–110.
- (99) The geometries for these complexes were constrained; the unconstrained complexes were also calculated, and the results are presented in the [Supporting Information](#). The regression equations differ slightly, but the conclusions drawn remain the same regardless of geometry constraints.
- (100) Bursten, B. E.; Chen, S.; Chisholm, M. H. *J. Organomet. Chem.* **2008**, *693*, 1547–1551.
- (101) Averkiev, B. B.; Truhlar, D. G. *Catal. Sci. Technol.* **2011**, *1*, 1526–1529.
- (102) This has been the subject of a study on Pd (ref 21). In future work, DFT calculations will be used to understand the extent to which these conclusions apply to reductive elimination from Pd(II) complexes.